



TITLE:

# Methylcelluloses end-functionalized with peptides as thermoresponsive supramolecular hydrogelators

AUTHOR(S):

Suhara, Ryo; Yamagami, Mao; Kamitakahara, Hiroshi; Yoshinaga, Arata; Tanaka, Yoshimasa; Takano, Toshiyuki

---

CITATION:

Suhara, Ryo ...[et al]. Methylcelluloses end-functionalized with peptides as thermoresponsive supramolecular hydrogelators. *Cellulose* 2019, 26(1): 355-382

ISSUE DATE:

2019-01

URL:

<http://hdl.handle.net/2433/242287>

RIGHT:

This is a post-peer-review, pre-copyedit version of an article published in *Cellulose*. The final authenticated version is available online at: <http://dx.doi.org/10.1007/s10570-018-2027-5>; この論文は出版社版ではありません。引用の際には出版社版をご確認ください。 ; This is not the published version. Please cite only the published version.

1 **Methylcelluloses End-Functionalized with**  
2 **Peptides as Thermoresponsive**  
3 **Supramolecular Hydrogelators**

4

5 Ryo Suhara<sup>†</sup>, Mao Yamagami<sup>†</sup>, Hiroshi Kamitakahara<sup>\*†</sup>, Arata Yoshinaga<sup>†</sup>,  
6 Yoshimasa Tanaka<sup>§</sup>, Toshiyuki Takano<sup>†</sup>

7 <sup>†</sup>*Graduate School of Agriculture, Kyoto University, Kitashirakawa-Oiwake-cho,*  
8 *Sakyo-ku, Kyoto 606-8502, Japan*

9 <sup>§</sup>*Center for Bioinformatics and Molecular Medicine, Graduate School of*  
10 *Biomedical Sciences, Nagasaki University, 1-12-4 Sakamoto, Nagasaki 852-8523,*  
11 *Japan*

12

13 **AUTHOR INFORMATION**

14 **Corresponding Author:** Hiroshi Kamitakahara

15 \*E-mail: [hkamitan@kais.kyoto-u.ac.jp](mailto:hkamitan@kais.kyoto-u.ac.jp); Tel: +81-75-753-6257

16 ORCID: Hiroshi Kamitakahara: 0000-0002-0130-1919

17

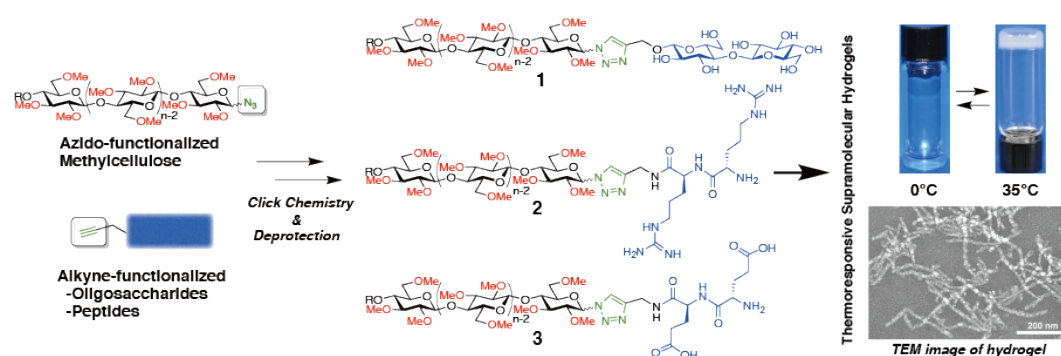
18 **Abstract** This paper describes the synthesis of methylcelluloses end-  
19 functionalized with peptides and an investigation into their functions. We found  
20 that aqueous solutions of methylcellulose end-functionalized not only with  
21 carbohydrates but also with peptide segments, such as di(arginine) and  
22 di(glutamic acid), behave as thermoresponsive supramolecular hydrogelators at  
23 human-body temperature. The slow drug release from thermoresponsive  
24 hydrogels of methylcelluloses end-functionalized with peptides is attributed to  
25 ionic interactions between model drugs and peptide segments in these hydrogels.  
26 Reactions of methylated cellobiose with di(arginine) and di(glutamic acid) were  
27 used to determine optimum reaction conditions for the synthesis of  
28 methylcelluloses end-functionalized with these peptide residues). The surface  
29 activities, zeta potentials, thermal properties, hydrogelation behavior, and  
30 cytotoxicities of these peptide-functionalized methylcelluloses are also discussed.

31

## Highlights:

- Methylcelluloses end-functionalized with peptides were synthesized.
- Peptides-end-functionalized methylcelluloses behave as thermoresponsive supramolecular hydrogelators at human-body temperature.
- The slow drug release from thermoresponsive hydrogels of methylcelluloses end-functionalized with peptides was achieved.

## Graphical Abstract:





## 42 Introduction

43 Thermoresponsive hydrogels have received increased attention in recent years.  
44 In particular, thermoresponsive supramolecular hydrogels (Du et al. 2015) with  
45 lower critical solution temperatures (LCSTs) (Yamagami et al. 2018) enable the  
46 development of biomedical applications such as injectable drug-delivery  
47 technology (Baumann et al. 2009). While poly(*N*-isopropylacrylamide)  
48 (Fundueanu et al. 2009) is a well known thermoresponsive polymer derived from  
49 fossil resources, methylcellulose (MC) is a thermoresponsive material from  
50 renewable resources.

51 The degree of substitution (DS) of industrially produced MC is 1.8, and its  
52 aqueous solution exhibits thermoreversible hydrogelation at approximately 60 °C.  
53 The physical properties of aqueous MC solutions have received considerable  
54 academic attention (Desbrieres et al. 1998; Heymann 1935; Rees 1972; Savage  
55 1957). Kato et al. concluded that the network junction points in MC gels are  
56 between 4 and 8 units long (Kato et al. 1978).

57 Our studies have focused on structure-property-function relationships of  
58 methylcellulose (Kamitakahara et al. 2009a; Kamitakahara et al. 2009b;  
59 Kamitakahara et al. 2008a; Kamitakahara et al. 2012; Kamitakahara and  
60 Nakatsubo 2010; Kamitakahara et al. 2006; Kamitakahara et al. 2007;  
61 Kamitakahara et al. 2009c; Kamitakahara et al. 2008b; Karakawa et al. 2002;  
62 Nakagawa et al. 2011a; Nakagawa et al. 2011b; Nakagawa et al. 2012a;  
63 Nakagawa et al. 2012b; Nakagawa et al. 2012c). Diblock methylcellulose bearing  
64 a sequence of at least ten 2,3,6-tri-*O*-methylglucosyl units and an unmodified  
65 cellobiosyl unit plays a crucial role in the thermoreversible hydrogelation of an  
66 aqueous MC solution (Nakagawa et al. 2011a).

67 Our detailed study on the structure-property relationships of methylcellulose  
68 with a sequence of over twenty 2,3,6-tri-*O*-methylglucosyl units revealed the  
69 thermoreversible hydrogelation properties of an aqueous diblock methylcellulose  
70 solution at human-body temperature (Nakagawa et al. 2011a). In addition, Bodvik  
71 et al. reported that MC forms fibrillar aggregates that were observed by cryogenic  
72 transmission electron microscopy (Cryo-TEM) (Bodvik et al. 2010); we also  
73 reported the same morphology (Nakagawa et al. 2012c), as did the group of  
74 Lodge (Lott et al. 2013a; Lott et al. 2013b). Moreover, we found that well-defined  
75 diblock methylcellulose self-assembles thermoresponsively into ribbon-like  
76 nanostructures in water to form a thermoreversible hydrogel at human-body  
77 temperature (Nakagawa et al. 2012c). The intermolecular interactions in the  
78 fibrillar nanostructure of commercial MC in aqueous solution at LCST and in the  
79 ribbon-like nanostructure of well-defined diblock methylcellulose are essentially  
80 the same; hydrophobic interactions between a sequence of 2,3,6-tri-*O*-  
81 methylglucosyl units, and hydrogen bonding between less-methylated glucosyl  
82 units both play crucial roles during the aggregation of methylcellulose molecules  
83 at LCST.

84 This finding prompted us to explore methylcellulose analogues that can be  
85 synthesized by more simple and straightforward methods than glycosylation  
86 (Nakagawa et al. 2011b). We selected the Huisgen 1,3-dipolar cycloaddition  
87 reaction for the development of methylcellulose analogues (Nakagawa et al.  
88 2012b). An aqueous solution of the newly synthesized methylcellulose analogue,  
89 which included hydrophobic and hydrophilic segments connected by 1,2,3-  
90 triazoles, exhibited thermoreversible hydrogelation properties (Nakagawa et al.  
91 2012b) equivalent to that of a well-defined diblock methylcellulose (Nakagawa et  
92 al. 2011b). Consequently, we developed a synthetic method for the end-

93 functionalization of methylcellulose to produce methylcellulosyl azide and  
94 propargyl methylcelluloside (Kamitakahara et al. 2016). Moreover, not only did  
95 nonionic segments, such as cellobiosyl units (as hydrophilic blocks) induce  
96 thermoreversible hydrogelation, but ionic segments did as well (Yamagami et al.  
97 2018), although it was crucial that the concentrations of the diblock  
98 methylcellulose analogues in aqueous media remain at 4 wt%.

99 Our recent results suggested that it might be possible to install any functional  
100 group at the methylcellulose end and retain thermoreversible hydrogelation  
101 behavior at human-body temperature. Hence, we explored the end-  
102 functionalization of methylcellulose with peptides. Peptides exhibit potent  
103 biological activities due to the functional diversity of their amino-acid chains, and  
104 play crucial roles in organisms that differ from those of oligo- and  
105 polysaccharides. Therefore, the end-functionalizations of polysaccharide  
106 derivatives with peptides are expected to yield a variety of functional materials  
107 that exhibit thermoresponsive properties. An oligosaccharide-based synthetic  
108 glycoprotein (Bonduelle and Lecommandoux 2013) has been reported by the  
109 group of Lecommandoux. However, polysaccharide-derivative-*block*-  
110 oligosaccharides (Breitenbach et al. 2017; de Medeiros Modolon et al. 2012) or  
111 polysaccharide-derivative-*block*-oligopeptides have not received much attention  
112 from researchers. Carbohydrate-based block copolymers with polyester (Fajardo  
113 et al. 2014; Liu and Zhang 2007), poly(methyl methacrylate) (Dax et al. 2013;  
114 Togashi et al. 2014), poly(styrene) (Loos and Müller 2002; Otsuka et al. 2013;  
115 Yagi et al. 2010), poly(*N*-isopropylacrylamide) (Dax et al. 2013; Otsuka et al.  
116 2012), poly( $\gamma$ -benzyl-L-glutamate) (Kamitakahara et al. 2014), and poly(3-  
117 hexylthiophene) (Sakai-Otsuka et al. 2017) polyisoprene (Hung et al. 2017), and  
118 poly(ethyleneoxide) (Akiyoshi et al. 1999) have been reported. Shoichet and her

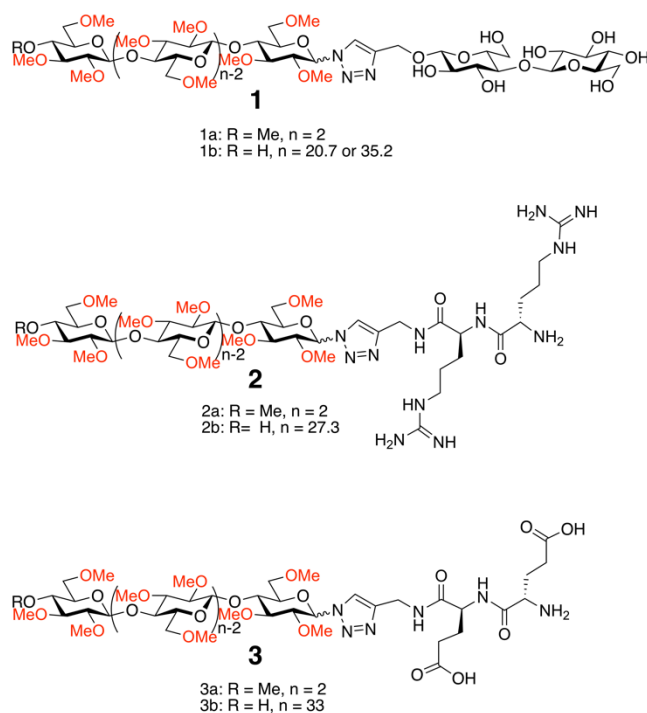
119 colleagues focused on a physical blend of hyaluronan and methylcellulose  
120 covalently linked to peptides for tissue-engineering purposes (Parker et al. 2016).  
121 They modified methylcellulose with peptides by the "grafting to" method, in  
122 which peptide moieties were randomly introduced onto the methylcellulose  
123 backbone. In contrast, our method gives thermoresponsive hydrogels composed of  
124 only methylcellulose and peptides, and are devoid of other polysaccharides. Our  
125 new peptide-end-functionalized methylcelluloses are linear polysaccharide  
126 derivatives with blocky structures that exhibit a broad range of new properties,  
127 including thermoreversible hydrogelation at temperatures close to that of the  
128 human body, formation of ribbonlike supramolecular nanostructures by self-  
129 assembly, surface activities, and slow drug release from thermoresponsive  
130 supramolecular hydrogel.

131 Herein, we describe the end-functionalization of tri-*O*-methylcellulose with  
132 cationic di(arginine) and anionic di(glutamic acid) units as peptide segments in  
133 order to develop new functionality (Chart 1). The synthesis, characterization, and  
134 thermal properties of aqueous solutions of these materials, as well as their zeta  
135 potentials, surface activities, in vitro cytotoxicities, and drug-release behavior  
136 from their supramolecular hydrogel matrices, are discussed.

137

138

139 **Chart 1. Compounds 1–3.**



140

141

142 **Results and discussion**

143 **Synthesis of Peptide Segments**

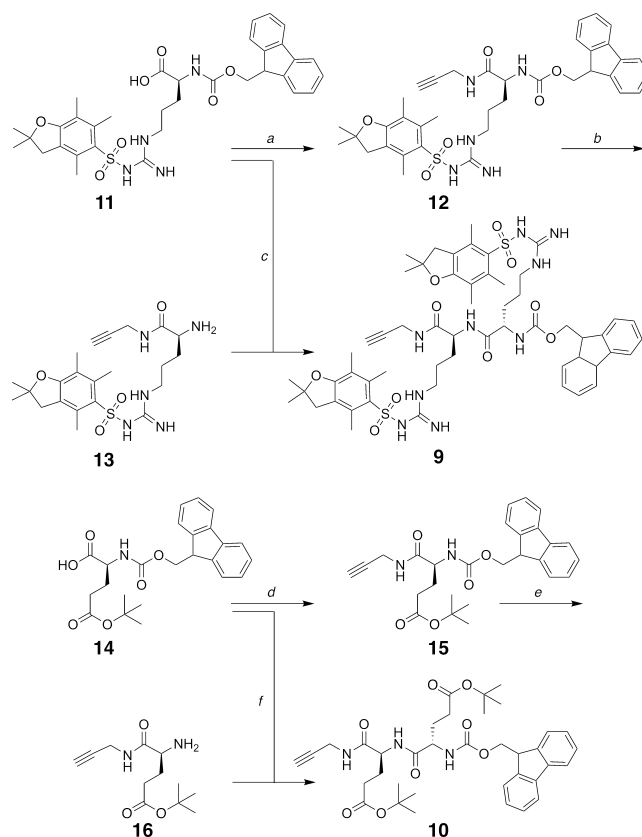
144 Peptide segments were synthesized following standard Fmoc methodology, as  
145 shown in Scheme 1. For side-chain protection, we used the 2,2,4,6,7-  
146 pentamethyldihydrobenzofuran-5-sulfonyl (pbf) group for the guanidine group,  
147 while the  $\gamma$  carboxylic acid group of glutamic acid was protected as a *tert*-butyl  
148 (*t*Bu) ester.

149 Propargylamine was reacted with *N* $\alpha$ -Fmoc-*N* $\omega$ -Pbf-L-arginine (**11**) to give the  
150 alkyne-functionalized *N* $\alpha$ -Fmoc-*N* $\omega$ -Pbf-L-arginine-*N*-propargylamide (**12**) in  
151 89% yield. The amide bond was successfully formed with DMT-MM (Kunishima  
152 et al. 1999a; Kunishima et al. 1999b) as the condensation reagent. The Fmoc  
153 group of compound **12** was removed to afford *N* $\omega$ -Pbf-L-arginine-*N*-

propargylamide (**13**) in 82% yield. *N*α-Fmoc-*N*ω-Pbf-L-arginine (**11**) was coupled with *N*ω-Pbf-L-arginine-*N*-propargylamide (**13**) to produce *N*α-Fmoc-*N*ω-Pbf-L-arginine-*N*ω-Pbf-L-arginine-*N*-propargylamide (**9**) in 89% yield.

Fmoc-Glu(*O**t*-Bu)-OH (**14**) was also reacted with propargylamine to produce the alkyne-functionalized Fmoc-Glu(*O**t*-Bu)-*N*-propargylamide (**15**) in quantitative yield. Removal of the Fmoc group from compound **15** afforded Glu(*O**t*-Bu)-*N*-propargylamide (**16**) in quantitative yield. Compounds **14** and **16** were coupled with DMT-MM to produce *N*α-Fmoc-Glu(*O**t*-Bu)-Glu(*O**t*-Bu)-*N*-propargylamide (**10**) in 95% yield.

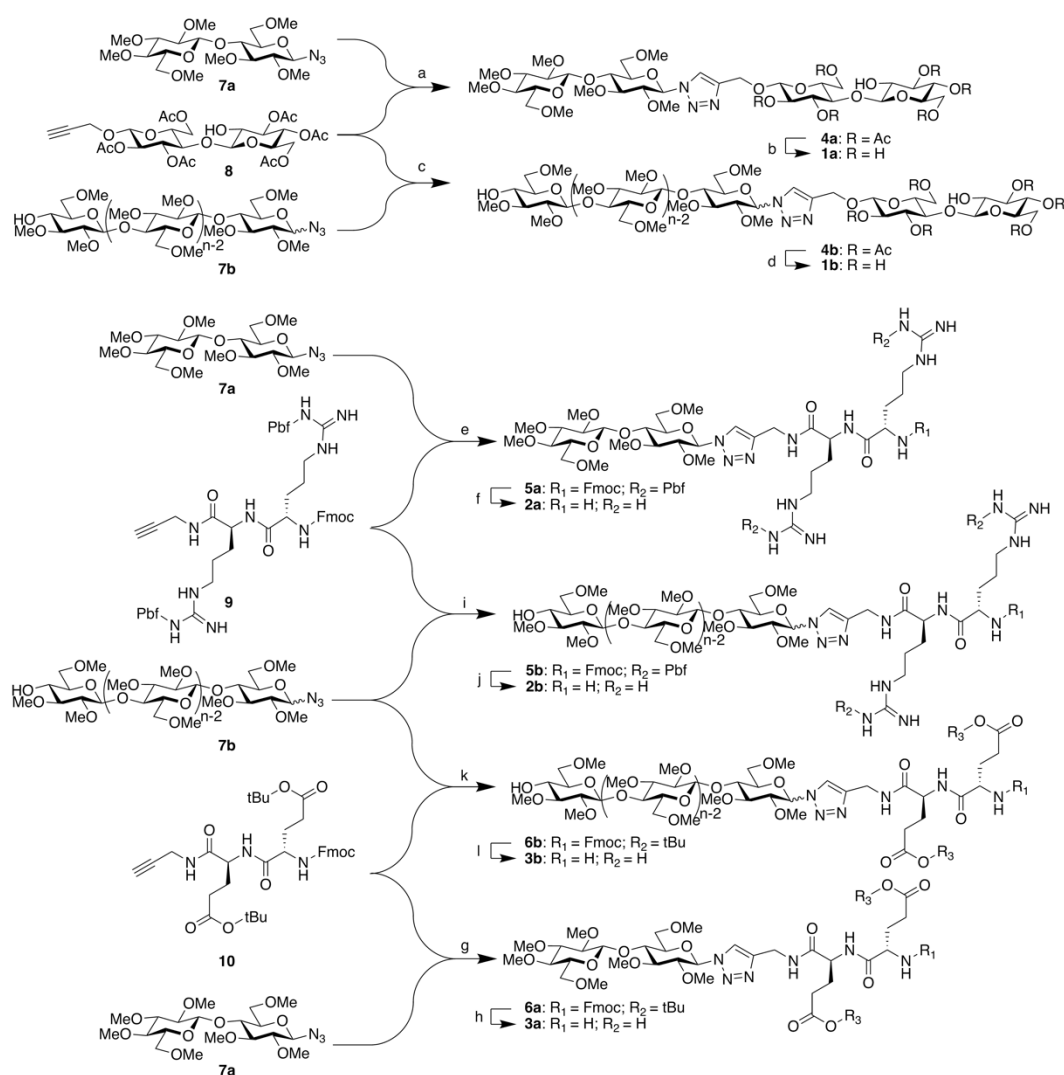
Compounds **9** and **10**, bearing alkyne groups, are peptide-containing segments for the end-functionalization of methylcellulose.



**Scheme 1.** Synthesis of peptide segments **9** and **10**. (a) propargylamine / DMT-MM / MeOH / r.t. / 3 h / 89%; (b) piperidine/CH<sub>2</sub>Cl<sub>2</sub> / r.t. / 1 / 82%; (c) DMT-MM / MeOH / r.t. / 4 h / 89%; (d) propargylamine / DMT-MM / MeOH / r.t. 3 h / quantitative yield; (e) piperidine/CH<sub>2</sub>Cl<sub>2</sub> / r.t. / 1 h / quantitative yield; (f) DMT-MM / MeOH / r.t. / 1 h / 95%.

## Peptide-End-Functionalized Methylcelluloses by Huisgen 1,3-Dipolar Cycloadditions

Scheme 2 displays the synthetic routes to methylcelluloses end-functionalized with peptides, as well as the control compounds. Trehalose-type methylated cellobiose derivative **1a** and diblock methylcellulose analogues **1b** (Yamagami et al. 2018) are control compounds for peptide-functionalized methylated cellobiose derivatives **2a** and **3a**, and peptide-end-functionalized methylcelluloses **2b** and **3b**, respectively.



**Scheme 2.** Synthesis of methylcelluloses end-functionalized with peptides

a) Cu(I)Br / sodium ascorbate / PMDETA / DMF / r.t. / 21 h / 56%; b) 28% NaOCH<sub>3</sub> in MeOH / MeOH/THF / r.t. / 3 h / quantitative yield; c) CuBr / sodium ascorbate / PMDETA / MeOH/CH<sub>2</sub>Cl<sub>2</sub> / r.t. / 4 d / 78.5%; d) 28% NaOCH<sub>3</sub> in MeOH / MeOH/THF / r.t. / overnight / quantitative yield; e) Cu(I)Br / sodium ascorbate / MeOH/CH<sub>2</sub>Cl<sub>2</sub> / r.t. / 2 h / 85%; f) piperidine /

185 CH<sub>2</sub>Cl<sub>2</sub> / r.t. / 1 h / 65%; TFA/H<sub>2</sub>O / 37 °C / 4 h / 52%; g) CuBr / sodium ascorbate / MeOH /  
186 CH<sub>2</sub>Cl<sub>2</sub> / r.t. / 2 h / 87%; h) piperidine / CH<sub>2</sub>Cl<sub>2</sub> / r.t. / 1 h / 47%; TFA/H<sub>2</sub>O / r.t. / 4 h / 58%; i)  
187 CuSO<sub>4</sub>·H<sub>2</sub>O / sodium ascorbate / MeOH/CH<sub>2</sub>Cl<sub>2</sub> / r.t. / 14 h / quantitative yield; j)  
188 piperidine/CH<sub>2</sub>Cl<sub>2</sub> / r.t. / 4 h / 89%; TFA/H<sub>2</sub>O / 37 °C / 4 h / 76%; k) CuSO<sub>4</sub>·H<sub>2</sub>O / sodium ascorbate  
189 / MeOH/CH<sub>2</sub>Cl<sub>2</sub> / r.t. / 14 h / 93%; l) piperidine/CH<sub>2</sub>Cl<sub>2</sub> / r.t. / 4 h / 84%; TFA/H<sub>2</sub>O / r.t. / 4 h / 52%.

190

191 Methylated cellobiose derivatives **2a** and **3a** were prepared in order to optimize  
192 reaction conditions for the methylcellulose derivatives. Copper-assisted azide-  
193 alkyne cycloaddition (CuAAC, the “click reaction”) of 2,3,4,6-tetra-*O*-methyl-β-  
194 D-glucopyranosyl-(1→4)-2,3,6-tri-*O*-methyl-β-D-glucopyranosyl azide (**7a**) and  
195 propargylated peptide segments **9** and **10** afforded methylated cellobiose  
196 derivatives **5a** (85% yield) and **6a** (87% yield) bearing peptide residues,  
197 respectively. Subsequent deprotections of the peptide segments gave methylated  
198 cellobioses **2a** and **3a** end-functionalized with peptides.

199 The optimized reaction conditions for the cellobiose derivatives allowed us to  
200 synthesize the peptide-functionalized methylcelluloses **2b** and **3b**. The CuAAC  
201 reactions of tri-*O*-methylcellulosyl azide (**7b**) and propargylated peptide segments  
202 **9** and **10** afforded methylcelluloses **5b** and **6b** end-functionalized with protected  
203 peptides, respectively; deprotection of the peptide segments of these compounds  
204 afforded peptide-functionalized methylcelluloses **2b** and **3b**.

205 While tri-*O*-methylcellulosyl azide (**7b**) is a mixture of both α- and β-anomers,  
206 the cellobiosyl azide **7a** is only the β-anomer. Moreover, each methylcellulose  
207 derivative **7b**, **4b**, **5b**, **6b**, **1b**, **2b**, and **3b** bears a single hydroxyl group at the C-4  
208 position of its methylated glucosyl residue furthest from the azide. In contrast,  
209 cellobiosyl azide derivative **7a** has no such hydroxyl group. We have reported the  
210 synthesis of blockwise alkylated (1→4) linked trisaccharides, and found that the  
211 anomeric configuration between the hydrophobic and hydrophilic segments  
212 affects surface activity of the aqueous solution (Nakagawa et al. 2011c).

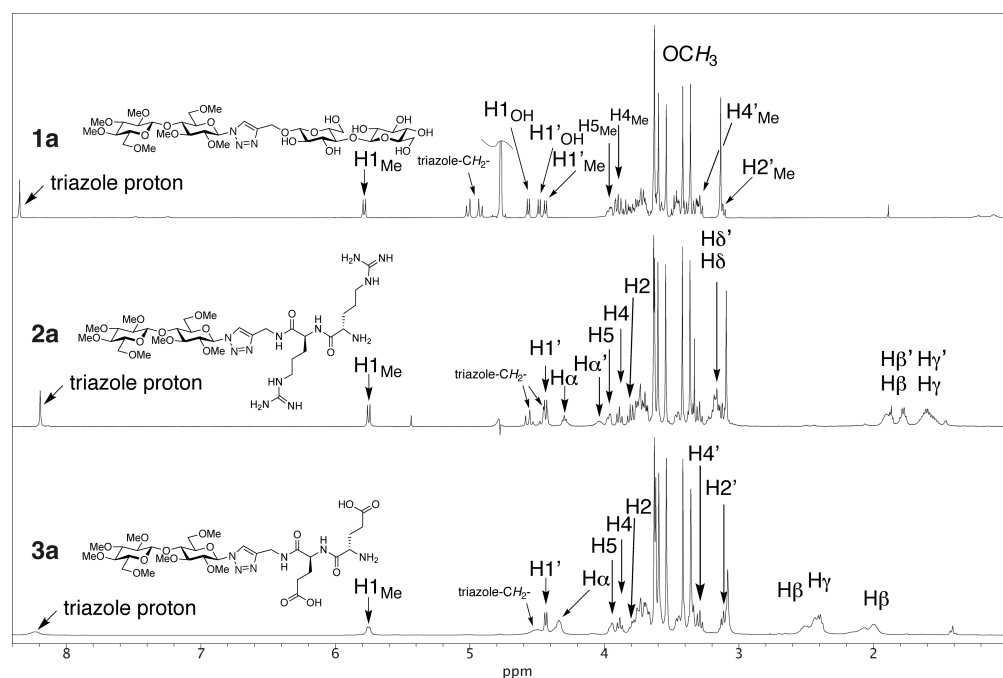


213

## 214 Characterization

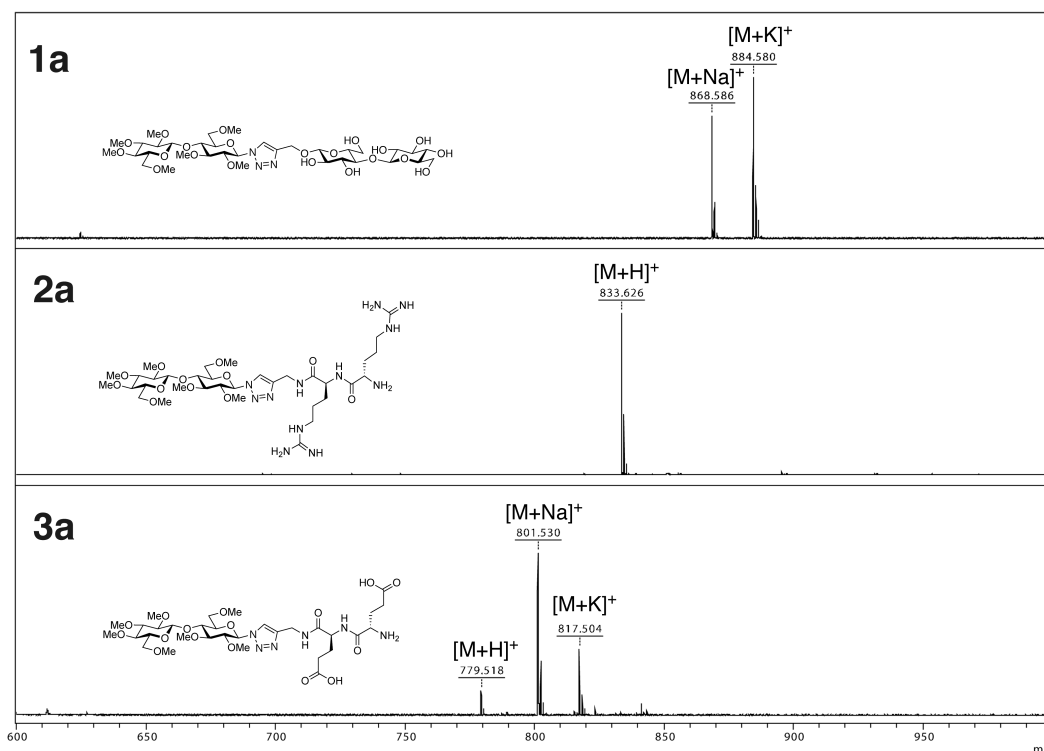
215 Figure 1 displays the  $^1\text{H}$ -NMR spectra of cellobiose derivatives **1a**, **2a**, and **3a**  
216 acquired in deuterium oxide. Proton resonances are assigned on the basis of two-  
217 dimensional NMR experiments (see experimental section). The triazole protons of  
218 compounds **1a**, **2a**, and **3a** appear at 8.24, 8.19, and 8.24 ppm, respectively.  
219 Carbon resonances of compounds **1a**, **2a**, and **3a** have also been assigned (see  
220 experimental section). Interestingly, the triazole proton of compound **3a** appears  
221 as a broad singlet. The methylene protons of compound **3a** adjacent to the triazole  
222 ring also appear as a broad peak at about 4.40–4.61 ppm. In addition, the C-1  
223 proton of the cellobiosyl residue appears as a broad doublet at 5.75 ppm.

224 The transverse relaxation times  $T_2$ s of triazole proton and C1 proton adjacent to  
225 the triazole of anionic compound **3a** would be shorter than that of compounds **1a**  
226 and **2a**, although molecular weights of compounds **1a**, **2a**, and **3a** are similar. The  
227 transverse relaxation times  $T_2$ s of protons of an anionic surfactant, sodium  
228 dodecyl sulfate (SDS), depend on their positions;  $T_2$ s of the internal protons are  
229 shorter than that of methyl protons and methylene protons adjacent to the sulfate  
230 group (Yu et al. 2017). The transverse relaxation time  $T_2$ s of the protons of  
231 anionic compound **3a** showed the same tendency as the anionic surfactant, SDS.



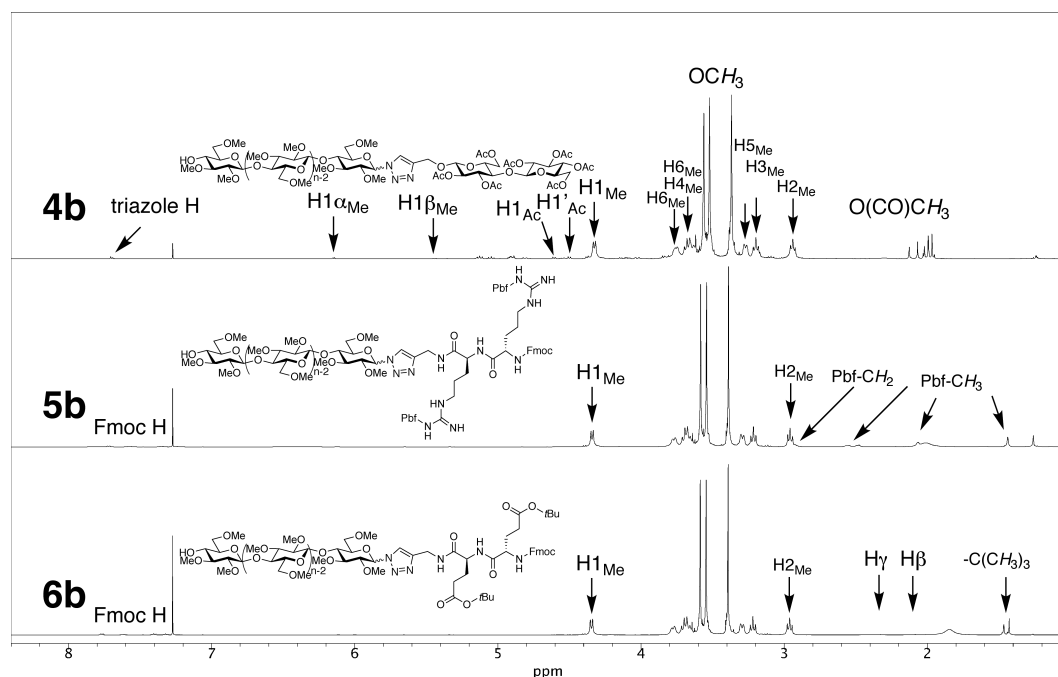
**Figure 1.** 500-MHz  $^1\text{H}$ -NMR spectra of compounds **1a**, **2a**, and **3a** in  $\text{D}_2\text{O}$ .

Figure 2 displays the MALDI-TOF MS spectra of compounds **1a**, **2a**, and **3a**. Pseudomolecular sodium  $[\text{M}+\text{Na}]^+$  and potassium  $[\text{M}+\text{K}]^+$  adduct-ion peaks corresponding to compound **1a** appear at  $m/z$  868.6 and 884.6, respectively. The pseudomolecular proton adduct-ion peak  $[\text{M}+\text{H}]^+$  of compound **2a** appears at  $m/z$  833.6, while pseudomolecular proton  $[\text{M}+\text{H}]^+$ , sodium  $[\text{M}+\text{Na}]^+$ , and potassium  $[\text{M}+\text{K}]^+$  adduct-ion peaks of compound **3a** appear at  $m/z$  779.5, 801.5, and 817.5, respectively.



**Figure 2.** MALDI-TOF MS spectra of compounds **1a**, **2a**, and **3a**.

In summary, the NMR and MALDI-TOF MS data for cellobiose derivatives **1a**, **2a**, and **3a** reveal that the conditions for the CuAAC reactions and the deprotections of the peptide residues are appropriate. Hence, the reaction conditions developed for these cellobiose derivatives were used to synthesize the peptide-functionalized methylcelluloses **1b**, **2b**, and **3b**.



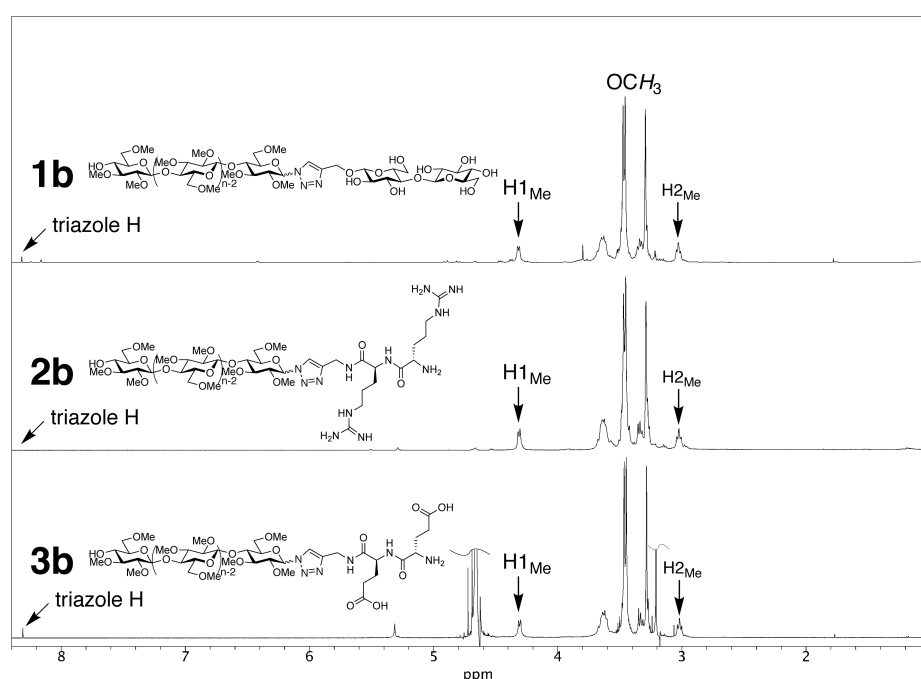
**Figure 3.**  $^1\text{H}$ -NMR spectra of compounds **4b**, **5b**, and **6b** in  $\text{CDCl}_3$ .

Compounds **5b** and **6b** as well as the trehalose-type diblock methylcellulose analogue **4b** (Yamagami et al. 2018), as an authentic sample of a methylcellulose end-functionalized with a peptide, were synthesized according to the optimized reaction conditions for cellobiose derivatives **5a** and **6a**, as well as **4a**. Figure 3 displays the  $^1\text{H}$ -NMR spectra of compounds **4b**, **5b**, and **6b** acquired in  $\text{CDCl}_3$ . The triazole proton of compound **4b** appears at 7.69 ( $\beta$ -anomer) and 7.70 ( $\alpha$ -anomer) ppm ( $\alpha/\beta$  ratio = 2/1) (Yamagami et al. 2018), while the triazole protons of compounds **5b** and **6b** were unable to be identified due to overlapping resonances associated with the aromatic protons of their Fmoc groups, although proton resonances of the peptide side-chains were observed.

The same deprotection procedures used for the cellobiosyl compounds **1a**, **2a**, and **3a** were used for the polymeric compounds, to give methylcellulose derivatives **1b**, **2b**, and **3b**. Figure 4 displays the  $^1\text{H}$ -NMR spectra of

267 methylcellulose derivatives **1b**, **2b**, and **3b** acquired in D<sub>2</sub>O. Resonances  
268 corresponding to the peptide moieties at the methylcellulose ends are not clearly  
269 evident in their spectra because of the higher DP of the methylcellulose residues,  
270 compared to the cellobiosyl compounds **1a**, **2a**, and **3a**, as shown in Figure 1.  
271 However, the triazole protons of compounds **2b** and **3b** appear at 8.42 and 8.43  
272 ppm, respectively, although those of compound **1a** appear at 8.42, 8.35, and 8.27  
273 ppm. This fact indicates that compounds **2b** and **3b** are end-functionalized with  
274 peptide residues. The zeta potential of compounds **1b**, **2b**, and **3b** summarized in  
275 Table 1 also indicate that the deprotections of compounds **2b** and **3b** were  
276 successful.

277

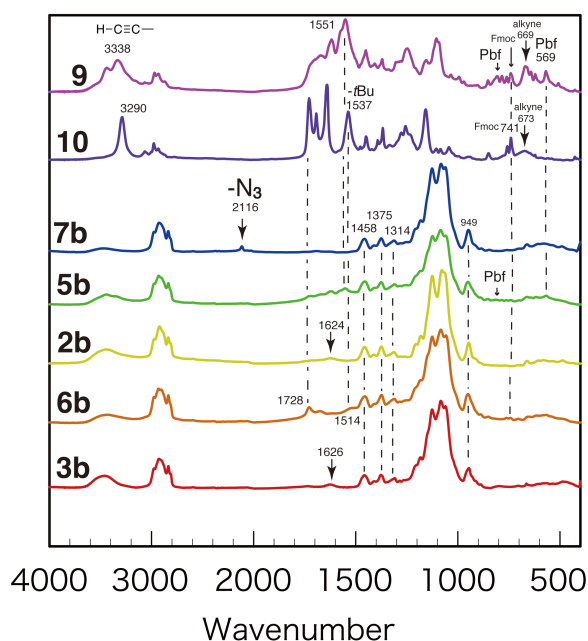


278 **Figure 4.** <sup>1</sup>H-NMR spectra of compounds **1b**, **2b**, and **3b** in D<sub>2</sub>O.

279

280 Figure 5 displays the FT-IR spectra of compounds **2b**, **3b**, **5b**, **6b**, **7b**, **9**, and **10**.  
281 Infrared absorption peaks corresponding to the protected di(arginine) and  
282 di(glutamic acid) segments **9** and **10** appear in the spectra of methylcelluloses **5b**

and **6b** end-functionalized with the di(arginine), and di(glutamic acid) derivatives, respectively. The infrared absorption peak associated with methylcellulosyl azide **7b** was observed at 2116 cm<sup>-1</sup>. After the Huisgen 1,3-dipolar cycloaddition of **7b** with the di(arginine) or di(glutamic acid) derivatives **9** or **10**, infrared absorption peaks associated with the azido group were not evident in the spectra of **5b** and **6b**, which indicates that the Huisgen 1,3-dipolar cycloadditions were successful. The infrared spectra of compounds **5b** and **6b** changed during deprotection to give **2b** and **3b**. The infrared absorption peaks corresponding to Pbf and Fmoc groups of MC-*b*-(Arg(Pbf))<sub>2</sub>-Fmoc **5b** were not evident in the spectrum of MC-*b*-ArgArg **2b**. The infrared absorption peaks associated with the *t*Bu and Fmoc groups of MC-*b*-(Glu(O*t*Bu))<sub>2</sub>-Fmoc **6b** were not evident in the spectrum of MC-*b*-GluGlu **3b**. The FT-IR analyses of the end-functionalized methylcellulose derivatives provide us with additional experimental data regarding the polymer reactions that occur at the ends of these macromolecules. We conclude that methylcelluloses **2b** and **3b** end-functionalized with peptides were successfully synthesized.



298

299 **Figure 5.** FT-IR spectra of compounds **2b**, **3b**, **5b**, **6b**, **7b**, **9**, and **10**.

## Physical properties of compounds **1b**, **2b**, and **3b**

Table 1 summarizes the structures, solution surface tensions, and zeta potentials of compounds **1b**, **2b**, and **3b**, while Figure 6 shows the surface tensions of solutions of compounds **1b**, **2b**, and **3b** as functions of concentration, measured at 23 °C. Compounds **2b** and **3b** exhibited similar surface-tension curves; the critical micelle concentrations (CMCs) of the arginine-containing compound **2b** and the glutamic-acid-containing compound **3b** are both 0.0035 mg/mL, slightly lower than that of the cellobiose derivative **1b** (0.008 mg/mL). An ionic peptide residue at the end of the methylcellulose unit improves its surface activity compared to that of methylcellulose end-functionalized with the nonionic cellobiosyl residue. In contrast, the CMCs of methylcelluloses **2b** and **3b** end-functionalized with peptides (0.0035 mg/mL) are clearly lower than that of commercial SM-4 methylcellulose (0.1 mg/mL).

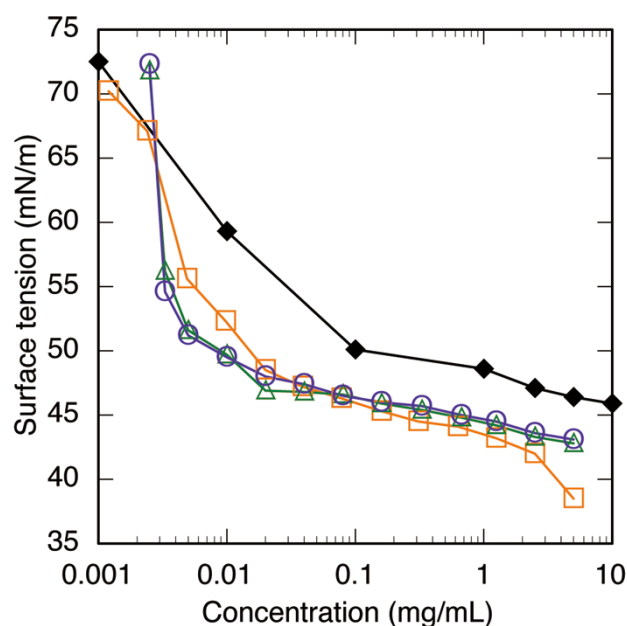


**Figure 6.** Surface tensions of compounds **1b**, (orange open squares), **2b** (green open triangles), and **3b** (purple open circles), and commercial MC (black solid diamonds), as functions of concentration.

317

318 **Table 1.** Surface tensions and zeta potentials of compounds **1b**, **2b**, and **3b**.

Comp. No.	Hydrophilic segment	$DP_n$ of hydrophobic segment	DS	Surface tension (mN/m) at CMC	Critical micelle concentration (mg/mL)	Zeta potential (mV)
<b>MC</b>			1.8	50.1	0.1	
<b>1b</b>	Cellobiose	20.7	2.65	49.0	0.008	-11.5
<b>2b</b>	Arginine dimer	27.3	–	47.3	0.0035	-7.5
<b>3b</b>	Glutamic acid dimer	32.8	–	49.3	0.0035	-14.1

319

320 Figure 7 displays the temperature-dependence of the supramolecular  
 321 aggregation behavior of compounds **1b**, **2b**, and **3b** in water, obtained by dynamic  
 322 light scattering (DLS) experiments. The hydrodynamic diameters of compounds  
 323 **1b**, **2b**, and **3b** at 25 °C were determined to be 138, 706, and 476 nm, respectively.  
 324 Although the hydrodynamic diameter of commercial MC SM-4 gradually  
 325 increased at temperatures above approximately 45 °C, those of compounds **1b**, **2b**,  
 326 and **3b** increased dramatically at 33 °C, 30 °C, and 31 °C, respectively.

327



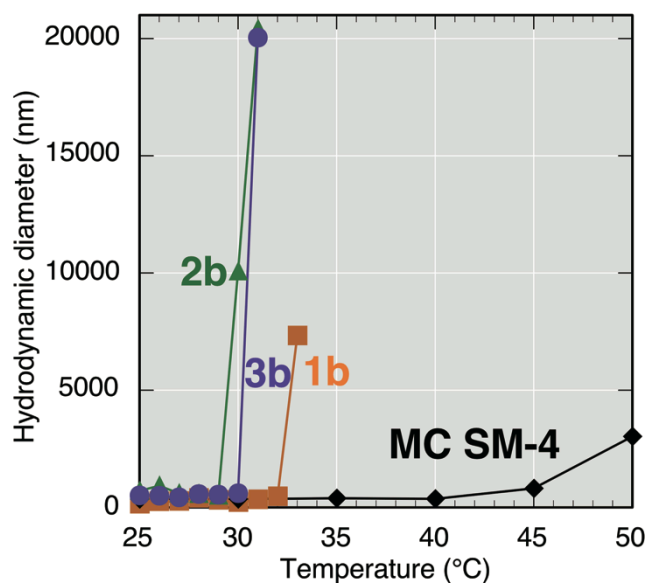


**Figure 7.** Hydrodynamic diameters of 0.2 wt% aqueous solutions of compounds **1b** (orange solid squares), **2b** (green solid triangles), **3b** (purple solid circles), and commercial MC (black solid diamonds) as functions of temperature.

331

Figure 8 shows the DSC thermograms of 2 wt% aqueous solutions of compounds **2b** and **3b**. Endothermic peaks appear at 31.5 °C and 32.6 °C for compounds **2b** and **3b**, respectively. The endothermic temperatures of compounds **2b** and **3b** are closely related to the supramolecular aggregation temperatures determined by DLS. The endothermic peaks observed by DSC are attributed to dehydration around the peptide-end-functionalized MCs **2b** and **3b**. Dehydration around these cellulosic molecules promotes their supramolecular aggregation, as shown in Figure 7.

340

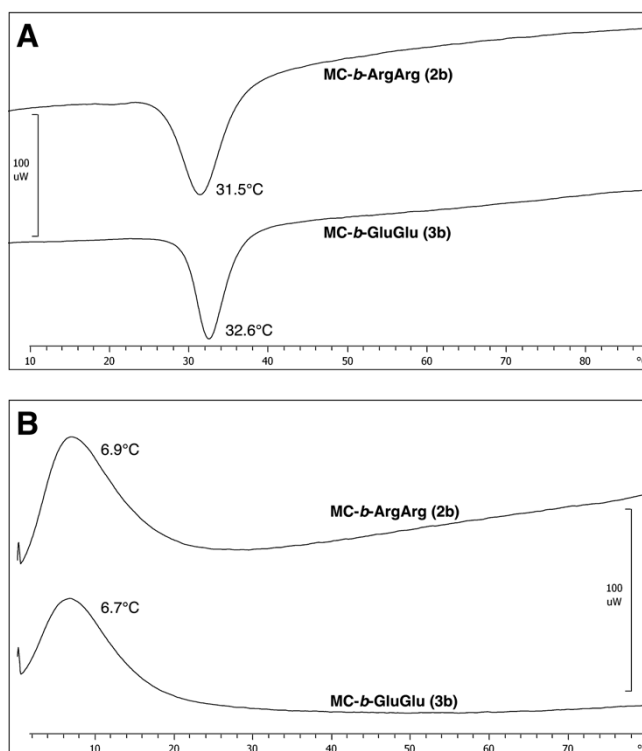
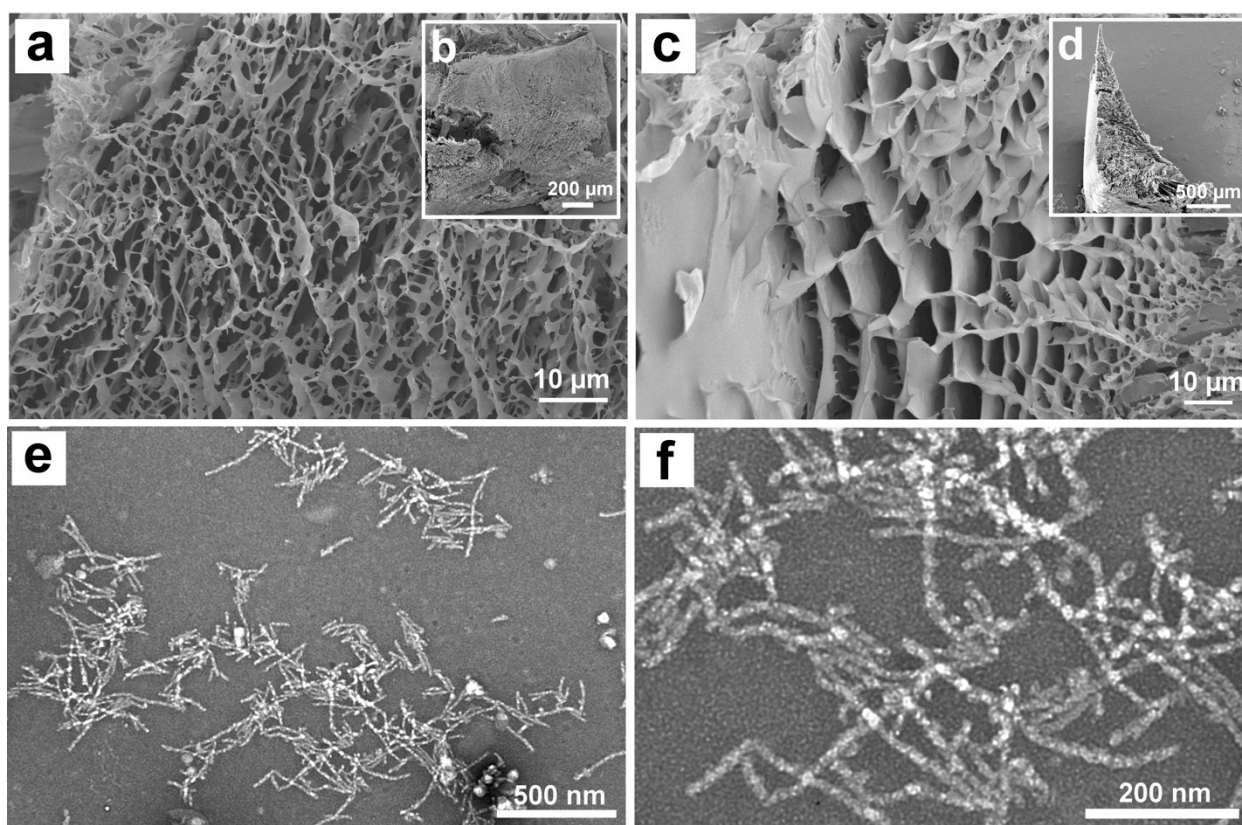


**Figure 8.** DSC thermograms of 2.0 wt% aqueous solutions of compounds **2b** and **3b**: (A) heating curves (3.5 °C/min) and (B) cooling curves (3.5 °C/min).

Table 2 displays images of 2.0 and 4.0 wt% aqueous solutions of compounds **1b**, **2b**, and **3b** at 0 and 35 °C. The 2 wt% aqueous solution of the cellobiose-functionalized MC **1b** forms a hydrogel at 35 °C. In contrast, the peptide-functionalized MCs **2b** and **3b** do not form hydrogels at 35 °C, rather their solutions became turbid at this temperature. In other words, the 2.0 wt% aqueous solutions of **2b** and **3b** phase separate at 35 °C. However, 4.0 wt% aqueous solutions of **1b**, **2b**, and **3b** form hydrogels at 35 °C. The concentrations of the thermally induced supramolecular structures of **2b** and **3b** are the keys to forming thermo-reversible hydrogels because 4.0 wt% aqueous solutions of the peptide-functionalized MCs **2b** and **3b** form hydrogels at 35 °C.

356 **Table 2.** Images of 2.0 and 4.0 wt% aqueous solutions of compounds **1b**, **2b**, and **3b**.

Comp. No.	Concentration: 2.0 wt %		Concentration: 4.0 wt %	
	Temperature (°C)		Temperature (°C)	
	0	35	0	35
<b>1b</b>				
<b>2b</b>				
<b>3b</b>				



357

358 **Figure 9.** SEM images of the hydrogels of (a, b) **2b** and (c, d) **3b**. (e, f) TEM images of the  
359 hydrogel of **2b**. Insets (b) and (d) are enlargements of regions in panels (a) and (c).

360

### 361 **Lyophilized hydrogels from compounds 2b and 3b**

362 SEM images of lyophilized hydrogels of **2b** and **3b** are shown in Figures 9a–d.  
363 We previously reported that methylcellulose end-functionalized with cellobiose  
364 exhibits a layered structure (Yamagami et al. 2018). In contrast, the peptide-  
365 functionalized methylcelluloses **2b** and **3b** form a three-dimensional mesh  
366 structure (**2b**) and a spongy, foam-like structure (**3b**), indicating that the  
367 hydrophilic segments at the ends of the methylcellulose units of the lyophilized  
368 hydrogels have different nanostructures.

### 369 **TEM images of the nanostructure of the thermoresponsive** 370 **supramolecular hydrogel of 2b**

371 TEM images of the hydrogel of compound **2b** are shown in Figures 9e–f, in  
372 which regular stick-like structures with orthogonal widths of approximately 12 nm  
373 and 15 nm, can be seen. The widths of the stick-like structures are constant,  
374 although their lengths vary widely. The molecular length of compound **2b** is ~16  
375 nm, which suggests that the longer width of a single rectangular structure is likely  
376 to correspond to the molecular length of compound **2b**. The average thickness of  
377 these structures was determined by atomic force microscopy to be approximately  
378 10 nm (data not shown). Rectangular self-assemblies appear to form stick-like  
379 structures, and their entanglements produce a macroscopic hydrogel.

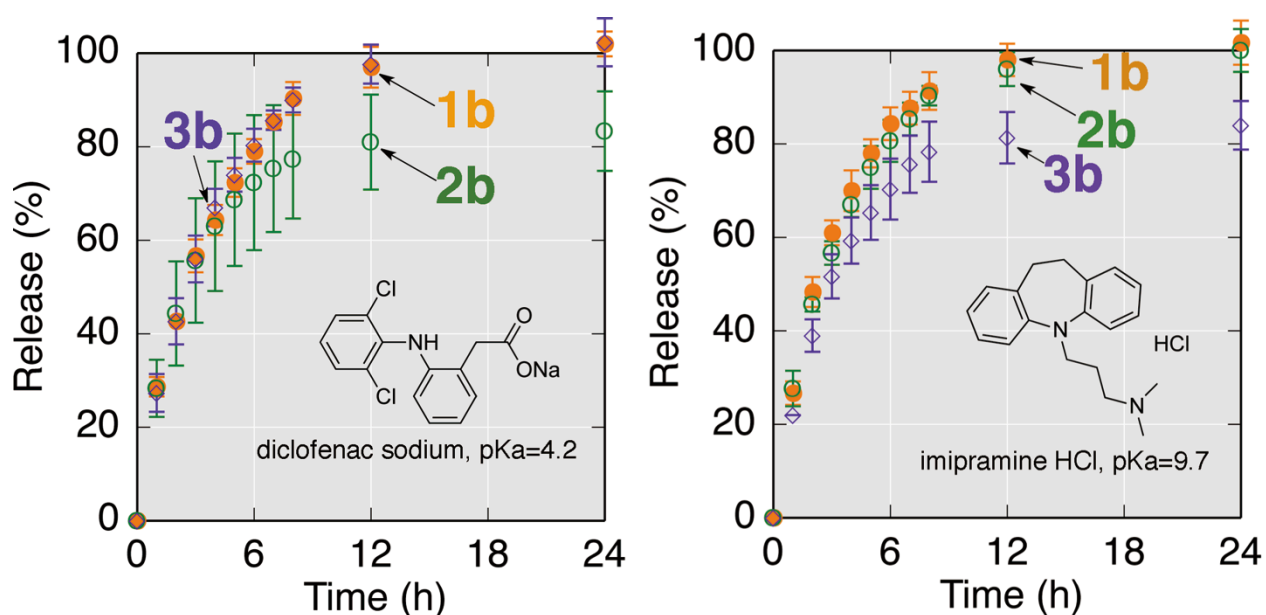
### 380 **Drug release from thermoresponsive supramolecular hydrogel** 381 **matrices**

382 The thermo-reversible supramolecular hydrogels of MCs **2b** and **3b** end-  
383 functionalized with cationic and anionic peptides, respectively, are expected to  
384 interact with anionic and cationic compounds, respectively. Therefore, we  
385 investigated the ionic drug-release behavior of these hydrogels. To that end,

diclofenac sodium and imipramine were selected as model anionic and cationic drugs, respectively.

Figure 10 displays the drug-release behavior of the thermoresponsive supramolecular hydrogel matrices of **1b**, **2b**, and **3b**. These matrices exhibit almost the same release behavior for diclofenac sodium (DFNa) at 37 °C at the start of release testing. Approximately 28–29% of the DFNa was released from hydrogel matrices **1b**, **2b**, and **3b** after 1 h. After 12 h, ~81% of the DFNa was released from cationic hydrogel matrix **2b**, while ~100% of the DFNa was released from the nonionic and anionic hydrogel matrices **1b** and **3b**. This observation indicates that the cationic di(arginine) segment at the end of the MC affects the release behavior of the anionic DFNa from the thermoresponsive supramolecular hydrogel matrix.

In contrast, cationic imipramine interacts with anionic supramolecular hydrogel matrix **3b**. At the beginning of imipramine-release testing (after 1 h of incubation) 27%, 28%, and 22% of the imipramine was released from hydrogel matrices **1b**, **2b**, and **3b**, respectively. After 12 h, 98%, 96%, and 81% of the imipramine was released from hydrogel matrices **1b**, **2b**, and **3b**, respectively, which indicates that the anionic di(glutamic acid) segment at the end of the MC interacts with the cationic imipramine. Ionic interactions between the cationic imipramine and the anionic hydrogel matrix **3b** promote the relatively slow release of imipramine from the thermoresponsive supramolecular hydrogel matrix.



407

408 **Figure 10.** Drug-release behavior from the thermoresponsive supramolecular hydrogel matrices of  
409 **1b** (orange solid circles), **2b** (green open circles), and **3b** (purple open diamonds).

410

411 To gain deep insight into the interaction between the model drugs and the MCs  
412 end-functionalized with peptides, we performed  $^1\text{H}$ -NMR experiments involving  
413 DFNa, methylated cellobiose derivative **2a** (a model compound of the MC end-  
414 functionalized with di(arginine) **2b**), and a mixture of DFNa and **2a**, in deuterium  
415 oxide.

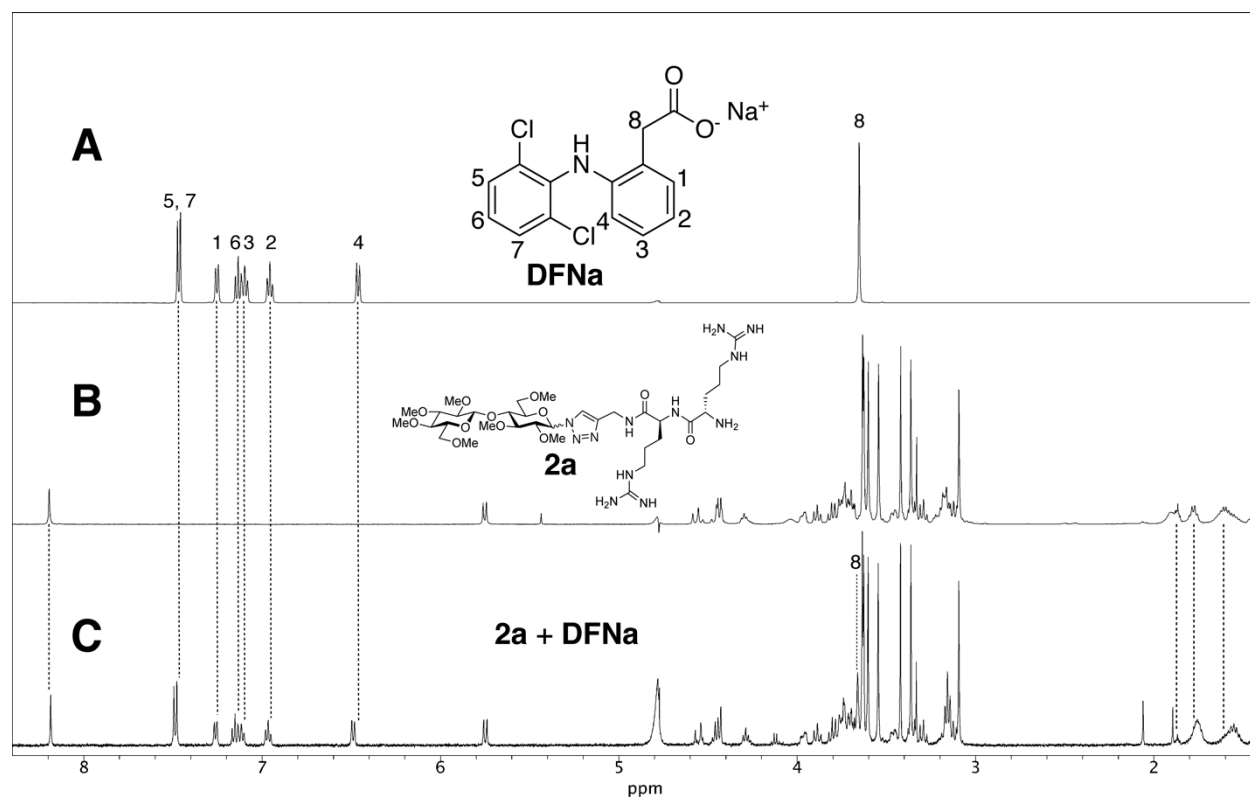
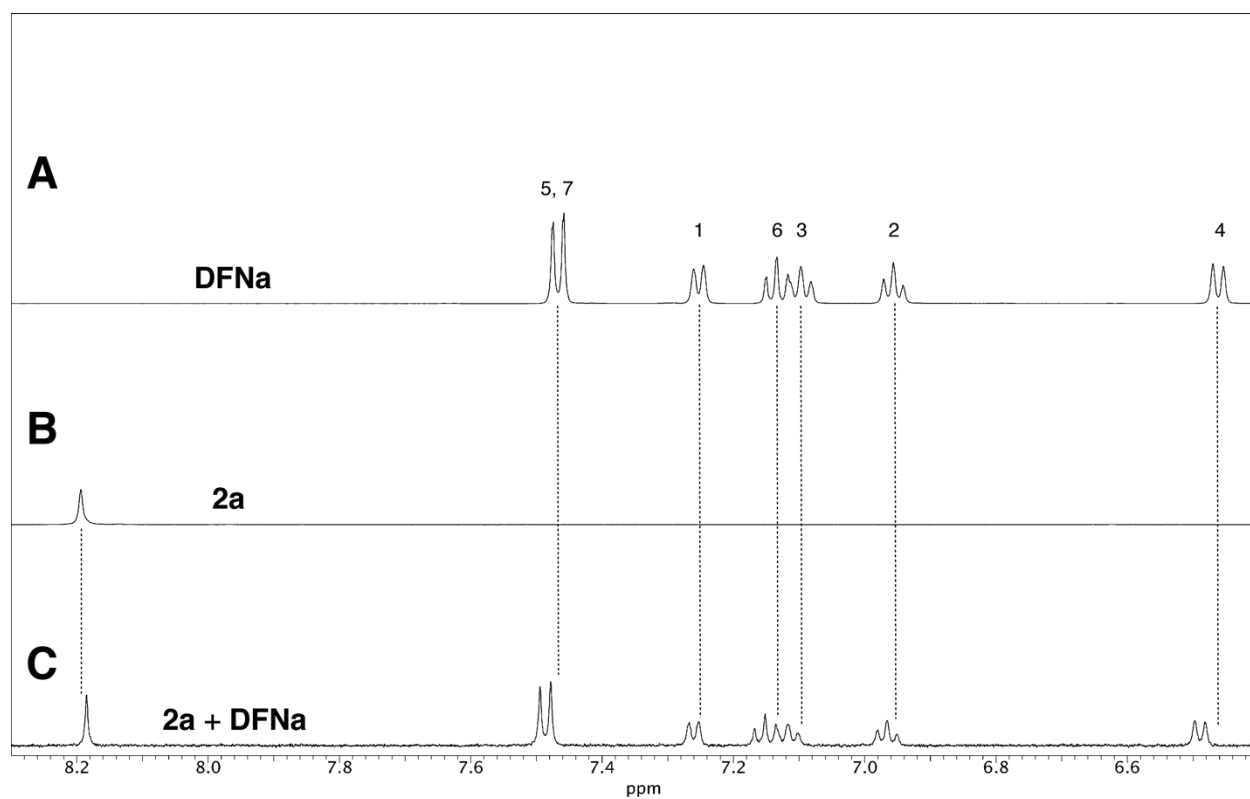
416 Figure 11 reveals changes in the chemical shifts corresponding to both  
417 compounds, namely DFNa and **2a**, following mixing. After mixing anionic DFNa  
418 and cationic **2a** in  $\text{D}_2\text{O}$ , the proton resonances of DFNa, numbered 1 to 8, were  
419 observed to shift downfield by 0.007, 0.010, 0.020, 0.033, 0.019, 0.019, 0.019,  
420 and 0.009 ppm, respectively, which indicates that all of the protons in DFNa  
421 became deshielded through the removal of electron density. In contrast, the  
422 methylene protons of the arginine side-chain appear at higher magnetic fields  
423 following mixing, which indicate that these protons have become shielded due to  
424 an increase in electron density. In addition, the triazole proton of **2a**, which

425 resonated at 8.19 ppm prior to mixing, also appeared at slightly higher magnetic  
426 field following mixing with DFNa.

427 These observations indicate that supramolecular hydrogels of methylcellulose  
428 end-functionalized with ionic peptides are expected to not only be  
429 thermoresponsive but also pH responsive. This temperature/pH dual-  
430 responsivenesses of compounds **2b** and **3b** are currently under investigation.

431





432 **Figure 11.**  $^1\text{H}$ -NMR analyses of the interactions between compound **2b** and diclofenac sodium.

433



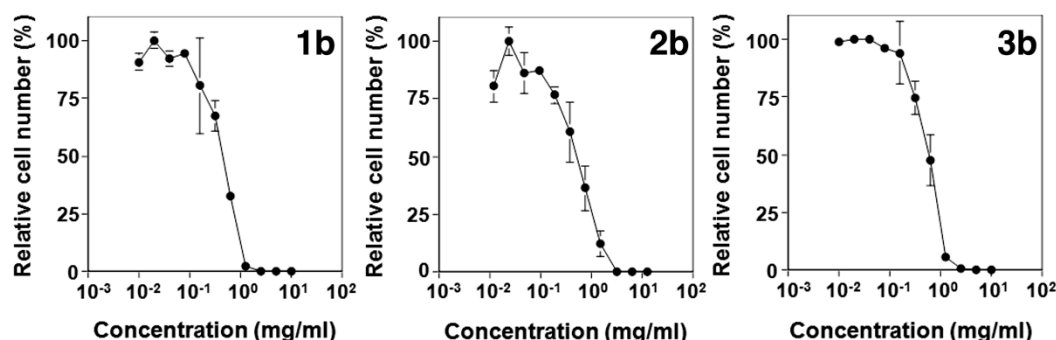


**Figure 12.** Inhibition of U937 cell growth by compounds **1b**, **2b**, and **3b**.

### Cytotoxicities of compounds **1b**, **2b**, and **3b**

ATP-based U937 histiocytoma cell-viability assays reveal that the half maximal inhibitory concentrations (IC<sub>50</sub> values) of compounds **1b**, **2b**, and **3b** were 470, 560, and 600 µg/mL, respectively, as shown in Figure 12. As previously noted, 4 wt% aqueous solutions (40 mg/mL) of compounds **2b** and **2c** become supramolecular thermoresponsive hydrogels at 37 °C (see Table 2). The hydrogelation of an aqueous solution of compound **2b** or **2c** is likely to inhibit cell growth of suspension-type cells such as U937. However, the cytotoxicities of aqueous solutions of compounds **2b** and **2c**, determined by IC<sub>50</sub> values, have been evaluated correctly, despite some supramolecular structures potentially present in the aqueous solutions. In summary, methylcelluloses end-functionalized with peptides are essentially nontoxic to U937 histiocytoma cells because IC<sub>50</sub> values of 0.6 wt% are considerably high.

### Conclusion

Aqueous solutions of methylcelluloses end-functionalized with peptides exhibit supramolecular thermoresponsive hydrogelation behavior equivalent to those of block-functionalization methylcelluloses (Nakagawa et al. 2011a; Nakagawa et al. 2012c; Yamagami et al. 2018). The tri-*O*-methylcellulose block, as a hydrophobic segment (Kamitakahara et al. 2016), is a key structure for supramolecular

thermoresponsive hydrogelation. Investigation into the relationships between the anomeric configuration at the reducing-end of the tri-*O*-methylcellulose block and physico-chemical properties in solution is now in progress. We were able to not only introduce carbohydrates (Yamagami et al. 2018) but also peptides as hydrophilic segments at the ends of hydrophobic tri-*O*-methylcellulose units, resulting in the syntheses of a pool of diblock methylcellulose analogues with biological functions that retain thermoresponsive hydrogelation behavior at human-body temperature. As methylcellulose is produced from cellulose, which is a natural resource, methylcelluloses end-functionalized with peptides are expected to be used in biomedical applications as, for example, comparatively safe injectable hydrogels.

467

## 468 **Experimental Section**

### 469 **Materials.**

470 *N*α-(9-Fluorenylmethoxycarbonyl)-*N*ω-(2,2,4,6,7-  
471 pentamethyldihydrobenzofuran-5-sulfonyl)-L-arginine (*N*α-Fmoc-*N*ω-Pbf-L-  
472 arginine) was purchased from Watanabe Chemical Industries, Ltd., Japan. *N*α-(9-  
473 Fluorenylmethoxycarbonyl)glutamic acid γ-tert-butyl ester monohydrate (Fmoc-  
474 Glu(*O**t*-Bu)-OH) was purchased from Peptide Institute, Inc., Japan. Other  
475 chemicals were purchased from Nacalai Tesque, Wako Pure Chemicals, Tokyo  
476 Chemical Industry, and Sigma-Aldrich. All reagents and solvents were of  
477 commercial grade and were used without further purification.

### 478 **Synthesis.**

479 *N*α-Fmoc-*N*ω-Pbf-L-arginine-*N*-propargylamide (12)

480 *N*α-Fmoc-*N*ω-Pbf-L-arginine-*N*-propargylamide (**12**) (Yang et al. 2011) was  
481 prepared from *N*α-Fmoc-*N*ω-Pbf-L-arginine (**11**) (89% yield). Briefly, to a  
482 solution of *N*α-Fmoc-*N*ω-Pbf-L-arginine (**11**, 200 mg) in methanol (5 mL) was  
483 added propargylamine (19 μL) and 4-(4,6-dimethoxy-1,3,5-triazin-2-yl)-4-  
484 methylmorpholinium chloride (DMT-MM, 102 mg). The reaction mixture was  
485 stirred for 3 h under nitrogen. The crude product was purified by preparative  
486 silica-gel thin-layer chromatography (PTLC, eluent: 10% MeOH/CH<sub>2</sub>Cl<sub>2</sub>) to give  
487 compound **12** (188 mg, 89% yield).

488 <sup>1</sup>H-NMR (500 MHz, CDCl<sub>3</sub>): δ 1.42 (6H, CH<sub>3</sub>, Pbf), 1.55-1.58 (m, 2H, H<sub>γ</sub>),  
489 1.85 (m, 2H, H<sub>β</sub>), 2.07 (s, 3H, CH<sub>3</sub>, Pbf), 2.14 (t, 1H, *J*=2.0 Hz, CH<sub>2</sub>CCH), 2.50  
490 (s, 3H, CH<sub>3</sub>, Pbf), 2.57 (s, 3H, CH<sub>3</sub>, Pbf), 2.91 (s, 2H, CH<sub>2</sub>, Pbf), 3.28 (m, 2H, H<sub>δ</sub>),  
491 3.98 (m, 2H, CH<sub>2</sub>CCH), 4.14 (t, 1H, *J*=7.0 Hz, CH, Fmoc), 4.27 (m, 1H, H<sub>α</sub>),  
492 4.34 (d, 2H, *J*=7.0 Hz, Fmoc), 7.24-7.74 (arom. Fmoc)

493 <sup>13</sup>C-NMR (125 MHz, CDCl<sub>3</sub>): δ 12.4 (CH<sub>3</sub>, Pbf), 17.9 (CH<sub>3</sub>, Pbf), 19.3 (CH<sub>3</sub>,  
494 Pbf), 25.2 (C<sub>γ</sub>), 28.5 (CH<sub>3</sub>, Pbf), 29.1 (CH<sub>2</sub>CCH), 30.1 (C<sub>β</sub>), 40.5 (C<sub>δ</sub>), 43.1 (CH<sub>2</sub>,  
495 Pbf), 46.9 (CH, Fmoc), 54.1 (C<sub>α</sub>), 67.1 (CH<sub>2</sub>, Fmoc), 71.3 (CH<sub>2</sub>CCH), 79.4  
496 (CH<sub>2</sub>CCH), 86.4 (C, Pbf), 117.5 (arom. Pbf), 119.9 (arom. Fmoc), 124.7 (arom.  
497 Pbf), 125.1 (arom. Fmoc), 127.0 (arom. Fmoc), 127.7 (arom. Fmoc), 132.3 (arom.  
498 Pbf), 138.4 (arom. Pbf), 141.1 (arom. Fmoc), 143.6 (arom. Fmoc), 143.7 (arom.  
499 Fmoc), 156.3, 156.6 (CO Fmoc, quaternary C of guanidino group of arginine),  
500 158.9 (-O-C<sub>α</sub> arom. Pbf), 172.1 (Arg, C<sub>α</sub>-CO-NH-)

#### 501 ***N*ω-Pbf-L-arginine-*N*-propargylamide (**13**)**

502 *N*α-Fmoc-*N*ω-Pbf-L-arginine-*N*-propargylamide (**12**, 200 mg) was dissolved in  
503 50% piperidine/dichloromethane (2 mL). The reaction mixture was stirred for 1 h  
504 at room temperature under nitrogen, after which it was concentrated to dryness.

505 The crude product was extracted with ethyl acetate, washed with water and brine,  
506 dried over sodium sulfate, and concentrated to dryness. The residue was purified  
507 by silica-gel column chromatography (eluent: 15% methanol/dichloromethane,  
508 v/v) to afford compound **13** (111 mg, 82% yield).

509 <sup>1</sup>H-NMR (500 MHz, CDCl<sub>3</sub>): δ 1.47 (6H, CH<sub>3</sub>, Pbf), 1.56-1.63 (m, 2H, H<sub>γ</sub>),  
510 1.80 (m, 2H, H<sub>β</sub>), 2.09 (s, 3H, CH<sub>3</sub>, Pbf), 2.22 (t, 1H, *J*=2.0 Hz, CH<sub>2</sub>CCH), 2.50  
511 (s, 3H, CH<sub>3</sub>, Pbf), 2.57 (s, 3H, CH<sub>3</sub>, Pbf), 2.96 (s, 2H, CH<sub>2</sub>, Pbf), 3.22 (m, 2H, H<sub>δ</sub>),  
512 3.45 (t, 1H, H<sub>α</sub>), 3.98 (m, 2H, CH<sub>2</sub>CCH),

513 <sup>13</sup>C-NMR (125 MHz, CDCl<sub>3</sub>): δ 12.4 (CH<sub>3</sub>, Pbf), 17.9 (CH<sub>3</sub>, Pbf), 19.3 (CH<sub>3</sub>,  
514 Pbf), 25.4 (C<sub>γ</sub>), 28.5 (CH<sub>3</sub>, Pbf), 28.8 (CH<sub>2</sub>CCH), 31.9 (C<sub>β</sub>), 40.6 (C<sub>δ</sub>), 43.2 (CH<sub>2</sub>,  
515 Pbf), 54.2 (C<sub>α</sub>), 71.3 (CH<sub>2</sub>CCH), 79.6 (CH<sub>2</sub>CCH), 86.4 (C, Pbf), 117.5 (arom.  
516 Pbf), 124.6 (arom. Pbf), 132.2 (arom. Pbf), 138.2 (arom. Pbf), 156.4 (quaternary  
517 C of guanidino group of arginine), 158.9 (-O-C arom. Pbf), 175.1 (Arg, C<sub>α</sub>-CO-  
518 NH-)

519 **N<sub>α</sub>-Fmoc-N<sub>ω</sub>-Pbf-L-arginine-N<sub>ω</sub>-Pbf-L-arginine-N-propargylamide (9)**  
520 (Morelli and Matile 2017)

521 To a solution of N<sub>α</sub>-Fmoc-N<sub>ω</sub>-Pbf-L-arginine (**11**, 101 mg, 1.2 equiv.) and N<sub>ω</sub>-  
522 Pbf-L-arginine-N-propargylamide (**13**, 60 mg, 1.0 equiv.) in methanol (5 mL) was  
523 added DMT-MM (43 mg, 1.2 equiv.). The reaction mixture was stirred for 4 h at  
524 room temperature under nitrogen, and then concentrated to dryness. The crude  
525 product was purified by PTLC (eluent: 10% methanol/dichloromethane) to afford  
526 compound **9** as colorless crystals (126 mg, 89% yield).

527 <sup>1</sup>H-NMR (500 MHz, CDCl<sub>3</sub>): δ 1.42 (12H, CH<sub>3</sub>, Pbf), 1.63 (m, 4H, H<sub>γ</sub>), 1.78  
528 (m, 2H, H<sub>β</sub>), 1.92 (m, 2H, H<sub>β</sub>), 2.05 (s, 3H, CH<sub>3</sub>, Pbf), 2.06 (s, 3H, CH<sub>3</sub>, Pbf),  
529 2.09 (1H, CH<sub>2</sub>CCH), 2.48 (s, 3H, CH<sub>3</sub>, Pbf), 2.49 (s, 3H, CH<sub>3</sub>, Pbf), 2.55 (s, 3H,

530 CH<sub>3</sub>, Pbf), 2.57 (s, 3H, CH<sub>3</sub>, Pbf), 2.90 (s, 2H, CH<sub>2</sub>, Pbf), 2.91 (s, 2H, CH<sub>2</sub>, Pbf),  
531 3.21 (m, 4H, H $\delta$ ), 3.91-3.96 (m, 2H, CH<sub>2</sub>CCH), 4.09 (t, 1H, *J*=7.0 Hz, CH, Fmoc),  
532 4.27 (broad t, 1H, H $\alpha$ ), 4.32-4.36 (d, d, 1H, 1H, *J*=7.0 Hz, Fmoc), 7.17-7.73  
533 (arom. Fmoc)  
534 <sup>13</sup>C-NMR (125 MHz, CDCl<sub>3</sub>):  $\delta$  12.4 (CH<sub>3</sub>, Pbf), 17.9 (CH<sub>3</sub>, Pbf), 19.3 (CH<sub>3</sub>,  
535 Pbf), 25.6 (C $\gamma$ ), 28.5 (CH<sub>3</sub>, Pbf), 29.1 (CH<sub>2</sub>CCH), 29.1 (C $\beta$ ), 40.0 (C $\delta$ ), 40.6 (C $\delta$ ),  
536 43.1 (CH<sub>2</sub>, Pbf), 46.9 (CH, Fmoc), 53.5 (C $\alpha$ ), 55.1 (C $\alpha$ ), 67.3 (CH<sub>2</sub>, Fmoc), 71.3  
537 (CH<sub>2</sub>CCH), 79.4 (CH<sub>2</sub>CCH), 86.4 (CH, Fmoc), 117.6 (arom. Pbf), 119.9 (arom.  
538 Fmoc), 124.7 (arom. Pbf), 125.1 (arom. Fmoc), 127.0 (arom. Fmoc), 127.7 (arom.  
539 Fmoc), 132.3 (arom. Pbf), 138.4 (arom. Pbf), 141.1 (arom. Fmoc), 143.7 (arom.  
540 Fmoc), 156.4, 157.0 (CO Fmoc, quaternary C of guanidino group of arginine),  
541 158.9 (-O-C arom. Pbf), 172.0 (Arg, C $\alpha$ -CO-NH-), 173.4 (Arg, C $\alpha$ -CO-NH-)  
542 MALDI-TOF MS (*m/z*): calcd for C<sub>56</sub>H<sub>73</sub>N<sub>9</sub>O<sub>10</sub>S<sub>2</sub>, 1095.49; found, [M+Na]<sup>+</sup> =  
543 1116.2  
544 FT-IR (KBr): 3440, 3338, 2970, 2934, 1670, 1618, 1551, 1450, 1369, 1248, 1155,  
545 1105, 853, 806, 783, 760, 741 (Fmoc), 669, 642, 621, 569 (Pbf, -SO<sub>2</sub>NH-) cm<sup>-1</sup>

546

547 **Fmoc-Glu(*Ot*-Bu)-*N*-propargylamide (15)** (Aagren et al. 2006)

548 To a solution of Fmoc-Glu(*Ot*-Bu)-OH (**14**, 300 mg) in methanol (5 mL) was  
549 added propargylamine (52  $\mu$ L) and DMT-MM (102 mg). The reaction mixture  
550 was stirred for 3 h under nitrogen. The crude product was purified by PTLC  
551 (eluent: 10% MeOH/CH<sub>2</sub>Cl<sub>2</sub>) to give compound **15** as colorless crystals (324 mg,  
552 quantitative yield).

553  $^1\text{H}$ -NMR (500 MHz,  $\text{CDCl}_3$ ):  $\delta$  1.47 (s, 9H,  $\text{CH}_3$ , *t*Bu), 1.96 (m, 1H,  $\text{H}\beta$ ), 2.09  
554 (m, 1H,  $\text{H}\beta$ ), 2.22 (t, 1H,  $J=2.0$  Hz,  $\text{CH}_2\text{CCH}$ ), 2.33 (m, 1H,  $\text{H}\gamma$ ), 2.43 (m, 1H,  
555  $\text{H}\gamma$ ), 4.05 (broad s, 2H,  $\text{CH}_2\text{CCH}$ ), 4.21 (2H, CH Fmoc,  $\text{H}\alpha$ ), 4.41 (m, 2H, Fmoc),  
556 5.78 (d, 1H,  $J=7.5$  Hz, NH), 6.70 (broad s, 1H, NH), 7.32 (dt, 2H,  $J=1.0$  Hz,  $J=7.5$   
557 Hz, Fmoc), 7.32 (dt, 2H,  $J=1.0$  Hz,  $J=1.0$  Hz, Fmoc), 7.41 (dt, 2H,  $J=1.0$  Hz,  
558 Fmoc), 7.77 (d, 2H,  $J=7.5$  Hz, Fmoc),

559  $^{13}\text{C}$ -NMR (125 MHz,  $\text{CDCl}_3$ ):  $\delta$  28.0 ( $\text{CH}_2\text{CCH}$ ), 28.0 ( $\text{CH}_3$ , *t*Bu), 39.2 ( $\text{C}\beta$ ),  
560 31.6 ( $\text{C}\gamma$ ), 47.1 ( $\text{CH}$ , Fmoc), 54.1 ( $\text{C}\alpha$ ), 67.1 ( $\text{CH}_2$ , Fmoc), 71.8 ( $\text{CH}_2\text{CCH}$ ), 79.1  
561 ( $\text{CH}_2\text{CCH}$ ), 81.2 (quaternary C of *t*Bu), 120.0 (arom. Fmoc), 125.0 (arom. Fmoc),  
562 127.1 (arom. Fmoc), 127.7 (arom. Fmoc), 141.3 (arom. Fmoc), 143.7 (arom.  
563 Fmoc), 156.3 (CO Fmoc), 171.0 (Glu,  $-\text{C}\alpha-\text{CO}-\text{NH}-$ ), 173.0 (Glu,  $\text{C}\delta\text{OO } t\text{Bu}$ )

564 MALDI-TOF MS ( $m/z$ ): calcd for  $\text{C}_{27}\text{H}_{30}\text{N}_2\text{O}_5$ , 462.22; found,  $[\text{M}+\text{Na}]^+ = 485.2$ ,  
565  $[\text{M}+\text{K}]^+ = 501.2$

566

567 **Glu(*Ot*-Bu)-*N*-propargylamide (16)** (Aagren et al. 2006)

568 Fmoc-Glu(*Ot*-Bu)-*N*-propargylamide (**15**, 308 mg) was dissolved in 50%  
569 piperidine/dichloromethane (2 mL). The reaction mixture was stirred for 1 h at  
570 room temperature under nitrogen, after which it was concentrated to dryness. The  
571 crude product was extracted with ethyl acetate, washed with water and brine,  
572 dried over sodium sulfate, and concentrated to dryness. The residue was purified  
573 by silica-gel column chromatography (eluent: dichloromethane; eluent: 5%  
574 methanol/dichloromethane, v/v) to afford compound **16** (166 mg, quantitative  
575 yield).

576  $^1\text{H}$ -NMR (500 MHz,  $\text{CDCl}_3$ ):  $\delta$  1.45 (s, 9H,  $\text{CH}_3$  (*t*Bu)), 1.83 (m, 1H,  $\text{H}\beta$ ), 2.09  
577 (m, 1H,  $\text{H}\beta$ ), 2.23 (t, 1H,  $J=2.0$  Hz,  $\text{CH}_2\text{CCH}$ ), 2.35 (m, 2H,  $\text{H}\gamma$ ), 3.44 (t, 1H,  $\text{H}\alpha$ ),  
578 4.05 (broad s, 2H,  $\text{CH}_2\text{CCH}$ ),

579  $^{13}\text{C}$ -NMR (125 MHz,  $\text{CDCl}_3$ ):  $\delta$  28.0 ( $\text{CH}_3$  (*t*Bu)), 28.8 ( $\text{CH}_2\text{CCH}$ ), 30.1 ( $\text{C}\beta$ ),  
580 31.9 ( $\text{C}\gamma$ ), 54.4 ( $\text{C}\alpha$ ), 71.4 ( $\text{CH}_2\text{CCH}$ ), 79.6 ( $\text{CH}_2\text{CCH}$ ), 80.7 ( $\text{C}(\text{CH}_3)_3$ ), 172.8  
581 (Glu,  $-\text{C}\alpha\text{-CO-NH-}$ ), 174.1 (Glu,  $\text{C}\delta\text{OO } t\text{Bu}$ )

582 MALDI-TOF MS ( $m/z$ ): calcd for  $\text{C}_{12}\text{H}_{20}\text{N}_2\text{O}_3$ , 240.15; found,  $[\text{M}+\text{Na}]^+ = 263.9$   
583

584 ***N* $\alpha$ -Fmoc-Glu(*Ot*-Bu)-Glu(*Ot*-Bu)-*N*-propargylamide (10)**

585 To a solution of Fmoc-Glu(*Ot*-Bu)-OH (**14**, 328 mg, 1.2 equiv.) and Glu(*Ot*-  
586 Bu)-*N*-propargylamide (**16**, 148 mg, 1.0 equiv.) in methanol (5 mL) was added  
587 DMT-MM (204 mg, 1.2 equiv.). The reaction mixture was stirred for 1 h at room  
588 temperature under nitrogen, and then concentrated to dryness. The crude product  
589 was purified by PTLC (eluent: 5% methanol/dichloromethane) to afford  
590 compound **10** as colorless crystals (378 mg, 95% yield).

591  $^1\text{H}$ -NMR (500 MHz,  $\text{CDCl}_3$ ):  $\delta$  1.43 (s, 9H,  $\text{CH}_3$  (*t*Bu)), 1.47 (s, 9H,  $\text{CH}_3$  (*t*Bu)),  
592 1.96-2.15 (m, 4H,  $\text{H}\beta$ ), 2.13 (t, 1H,  $J=2.0$  Hz,  $\text{CH}_2\text{CCH}$ ), 2.33-2.47 (m, 4H,  $\text{H}\gamma$ ),  
593 3.96-4.03 (broad s, 2H,  $\text{CH}_2\text{CCH}$ ), 4.20 (1H, H (Fmoc)), 4.20-4.24 (1H,  $\text{H}\alpha$ ),  
594 4.38-4.44 (m, 2H,  $\text{CH}_2$  (Fmoc)), 4.48-4.49 (m, 1H,  $\text{H}\alpha$ ), 7.30-7.77 (8H, arom.  
595 Fmoc)

596  $^{13}\text{C}$ -NMR (125 MHz,  $\text{CDCl}_3$ ):  $\delta$  27.0 ( $\text{C}\beta'$ ), 27.4 ( $\text{C}\beta$ ), 28.0 ( $\text{CH}_3$  (*t*Bu)), 29.1  
597 ( $\text{CH}_2\text{CCH}$ ), 30.1 31.7 ( $\text{C}\gamma'$ ), 31.8 ( $\text{C}\gamma$ ), 52.6 ( $\text{C}\alpha'$ ), 55.2 ( $\text{C}\alpha$ ), 67.3 ( $\text{CH}_2$ , Fmoc),  
598 71.3 ( $\text{CH}_2\text{CCH}$ ), 79.4 ( $\text{CH}_2\text{CCH}$ ), 81.1 ( $\text{C}(\text{CH}_3)_3$ ), 81.3 ( $\text{C}(\text{CH}_3)_3$ ), 120.0, 125.1,  
599 127.0, 127.7, 141.2, 143.7, 156.5, 170.6 (Glu,  $-\text{C}\alpha\text{-CO-NH-}$ ), 171.6 (Glu,  $-\text{C}\alpha\text{-}$   
600  $\text{CO-NH-}$ ), 173.0 (Glu,  $\text{C}\delta\text{OO } t\text{Bu}$ ), 173.2 (Glu,  $\text{C}\delta\text{OO } t\text{Bu}$ )

601 MALDI-TOF MS ( $m/z$ ): calcd for  $\text{C}_{36}\text{H}_{45}\text{N}_3\text{O}_8$ , 647.32; found,  $[\text{M}+\text{Na}]^+ = 670.4$

602 FT-IR (KBr): 3290, 2978, 1728, 1694, 1639, 1537 (*t*Bu), 1450, 1368, 1258,  
603 1157, 851, 758, 741 (Fmoc),  $673\text{ cm}^{-1}$

604

605     **2,3,4,6-Tetra-*O*-methyl- $\beta$ -D-glucopyranosyl-(1 $\rightarrow$ 4)-2,3,6-tri-*O*-methyl- $\beta$ -D-**  
606 **glucopyranosyl azide (**7a**)**

607     A 60% suspension of sodium hydride in mineral oil (1.97 g, 82.1 mmol, 14.0  
608 equiv.) was added to a solution of  $\beta$ -D-glucopyranosyl-(1 $\rightarrow$ 4)- $\beta$ -D-glucopyranosyl  
609 azide (Schamann and Schafer 2003; Ying and Gervay-Hague 2003) (1.29 g, 3.51  
610 mmol) in DMF (30 mL) at 0 °C. The mixture was stirred at 0 °C for 1 h under  
611 nitrogen. Methyl iodide (3.1 mL, 49.8 mmol, 14.2 equiv.) was then added to the  
612 reaction mixture at 0 °C. After 2 h, the mixture was warmed to room temperature  
613 and stirred for 2 h. The reaction was monitored by analytical thin-layer  
614 chromatography (TLC). Methanol (0.43 mL) was added to deactivate the sodium  
615 hydride. The mixture was concentrated and the crude product was extracted with  
616 ethyl acetate, washed with distilled water, brine, dried over Na<sub>2</sub>SO<sub>4</sub>, and  
617 concentrated to dryness. The residue was purified by silica-gel column  
618 chromatography (eluent: 2:1 (v/v) ethyl acetate/*n*-hexane) to give colorless  
619 crystals (**7a**, 0.799 g, 49% yield).

620     <sup>1</sup>H-NMR (500 MHz, CDCl<sub>3</sub>):  $\delta$  2.86 (dd, 1H, *J*=8.0 Hz, *J*=8.5 Hz, H2'), 1H,  
621 2.90 (t, 1H, *J*=9.0 Hz, H3'), 3.06 (t, 1H, *J*=9.5 Hz, H3'), 3.12 (t, 1H, *J*=9.5 Hz,  
622 H4'), 3.16 (ddd, 1H, *J*=2.0 Hz, *J*=4.0 Hz, *J*=9.5 Hz, H5'), 3.19 (t, 1H, *J*=9.0 Hz,  
623 H3), 3.32 (s, 3H, OCH<sub>3</sub>), 3.34 (s, 3H, OCH<sub>3</sub>), 3.36 (ddd, 1H, *J*=2.0 Hz, *J*=4.0 Hz,  
624 *J*=10.0 Hz, H5), 3.46 (s, 3H, OCH<sub>3</sub>), 3.48 (s, 3H, OCH<sub>3</sub>), 3.52 (dd, 1H, *J*=4.0 Hz,  
625 *J*=11.0 Hz, H6), 3.53 (s, 6H, OCH<sub>3</sub>), 3.56 (s, 3H, OCH<sub>3</sub>), 3.56 (dd, 1H, *J*=2.0 Hz,  
626 *J*=10.5 Hz, H6'), 3.62 (dd, 1H, *J*=9.0 Hz, *J*=10.0 Hz, H4), 3.63 (dd, 1H, *J*=2.0 Hz,  
627 *J*=11.0 Hz, H6), 3.67 (dd, 1H, *J*=4.0 Hz, *J*=11.0 Hz, H6), 4.23 (d, 1H, *J*=7.5 Hz,  
628 H1'), 4.40 (d, 1H, *J*=8.5 Hz, H1)



629  $^{13}\text{C}$ -NMR (125 MHz,  $\text{CDCl}_3$ ):  $\delta$  103.2 (C1'), 89.9 (C1), 86.9 (C3'), 84.9 (C3),  
630 84.0 (C2'), 82.8 (C2), 79.3 (C4'), 77.2 (C4), 76.9 (C5), 74.7 (C5'), 71.2 (C6'), 70.1  
631 (C6), 60.8, 60.6, 60.6, 60.6, 60.3, 59.3, 59.2 ( $\text{OCH}_3$ )

632

633 Tri-*O*-methylcellulosyl azide (**7b**) Compound **7b** was prepared according to our  
634 previous paper (Kamitakahara et al. 2016).

635 FT-IR (KBr): 3478, 2926, 2836, 2116 ( $\text{N}_3$ ), 1458, 1375, 1314, 1182, 1061, 949,  
636 664  $\text{cm}^{-1}$

637

638 **2-Propynyl 2,3,6-tri-*O*-acetyl- $\beta$ -D-glucopyranosyl-(1 $\rightarrow$ 4)-2,3,6-tri-*O*-acetyl-**  
639  **$\beta$ -D-glucopyranoside (8)** Compound **8** was prepared according to our previous  
640 paper (Yamagami et al. 2018).

641

642 **1-[2,3,4,6-Tetra-*O*-methyl- $\beta$ -D-glucopyranosyl-(1 $\rightarrow$ 4)-2,3,6-tri-*O*-methyl- $\beta$ -**  
643 **D-glucopyranosyl]-4-[2,3,4,6-tetra-*O*-acetyl- $\beta$ -D-glucopyranosyl-(1 $\rightarrow$ 4)-2,3,6-**  
644 **tri-*O*-acetyl- $\beta$ -D-glucopyranosyloxymethyl]-1*H*-1,2,3-triazole (4a)**

645 Azide **7a** (117 mg, 0.252 mmol) and glycoside **8** (170 mg, 0.252 mmol) were  
646 dissolved in DMF (9 mL). Copper(I) bromide (361.5 mg, 2.52 mmol, 10 equiv.),  
647 sodium ascorbate in water (998.5 mg/1.26 mL, 20 equiv.), and *N,N,N',N'',N'''*-  
648 pentamethyldiethylenetriamine (PMDETA, MW = 173.3,  $d$  = 0.83 g/mL, 0.5 mL,  
649 10 equiv.) were added to the solution at room temperature. The reaction mixture  
650 was stirred for 21 h. The insoluble component was then removed by filtration and  
651 washed with dichloromethane. The washings and filtrate were combined and  
652 concentrated, and the DMF was azeotropically removed with ethanol. The crude  
653 product was purified by silica-gel column chromatography (eluent: 10%

654 MeOH/CH<sub>2</sub>Cl<sub>2</sub>) to give 1-[2,3,4,6-tetra-*O*-methyl-β-D-glucopyranosyl-(1→4)-  
655 2,3,6-tri-*O*-methyl-β-D-glucopyranosyl]-4-[2,3,4,6-tetra-*O*-acetyl-β-D-  
656 glucopyranosyl-(1→4)-2,3,6-tri-*O*-acetyl-β-D-glucopyranosyloxymethyl]-1*H*-  
657 1,2,3-triazole (**4a**, 161.3 mg, 56% yield).

658 <sup>1</sup>H-NMR (500 MHz, CDCl<sub>3</sub>): δ 1.97, 1.99, 2.01, 2.01, 2.04, 2.09, 2.15 (COCH<sub>3</sub>),  
659 2.95 (t, 1H, *J*=8.5 Hz, H2'<sub>Me</sub>), 3.15 (t, 1H, *J*=9.0 Hz, H3'<sub>Me</sub>), 3.19 (s, 3H, OCH<sub>3</sub>),  
660 3.21 (t, 1H, *J*=9.0 Hz, H4'<sub>Me</sub>), 3.26 (ddd, 1H, *J*=2 Hz, *J*=3.5 Hz, *J*=9.5 Hz, H5'<sub>Me</sub>),  
661 3.33 (s, 3H, OCH<sub>3</sub>), 3.43 (s, 3H, OCH<sub>3</sub>), 3.44 (t, 1H, *J*=9.0 Hz, H3<sub>Me</sub>), 3.55 (s, 3H,  
662 OCH<sub>3</sub>), 3.57 (s, 3H, OCH<sub>3</sub>), 3.64 (s, 6H, OCH<sub>3</sub>), 3.6-3.7 (H6'<sub>Me</sub>, H2<sub>Me</sub>, H5<sub>Me</sub>, H5<sub>Ac</sub>,  
663 H5'<sub>Ac</sub>), 3.75 (dd, 1H, *J*=4.0 Hz, *J*=11.0 Hz, H6<sub>Me</sub>), 3.79 (t, 1H, *J*=9.5 Hz, H4<sub>Ac</sub>),  
664 3.82 (dd, 1H, *J*=9.0 Hz, *J*=10.0 Hz, H4<sub>Me</sub>), 4.05 (dd, 1H, *J*=2.5 Hz, *J*=12.5 Hz,  
665 H6<sub>Ac</sub>), 4.11 (dd, 1H, *J*=5.0 Hz, *J*=12.0 Hz, H6'<sub>Ac</sub>), 4.34 (d, 1H, *J*=8.0 Hz, H1'<sub>Me</sub>),  
666 4.36 (dd, 1H, *J*=4.0 Hz, *J*=12.0 Hz, H6<sub>Ac</sub>), 4.52 (d, 1H, *J*=8.0 Hz, H1'<sub>Ac</sub>), 4.56 (dd,  
667 1H, *J*=2.0 Hz, *J*=12.0 Hz, H6'<sub>Ac</sub>), 4.62 (d, 1H, *J*=8.0 Hz, H1<sub>Ac</sub>), 4.81 (d, 1H,  
668 *J*=13.0 Hz, OCH<sub>2</sub>-triazole), 4.92 (d, 1H, *J*=13.0 Hz, OCH<sub>2</sub>-triazole), 4.9-4.95  
669 (H2<sub>Ac</sub>, H2'<sub>Ac</sub>), 5.07 (t, 1H, *J*=9.5 Hz, H4'<sub>Ac</sub>), 5.15 (t, 1H, *J*=9.0 Hz, H3<sub>Ac</sub>), 5.15 (t,  
670 1H, *J*=9.0 Hz, H3'<sub>Ac</sub>), 5.47 (d, 1H, *J*=9.5 Hz, H1<sub>Me</sub>), 7.69 (s, 1H, triazole)

671 <sup>13</sup>C-NMR (125 MHz, CDCl<sub>3</sub>): δ 20.5, 20.6, 20.6, 20.9 (COCH<sub>3</sub>), 59.0 (OCH<sub>3</sub>),  
672 59.4 (OCH<sub>3</sub>), 60.3 (OCH<sub>3</sub>), 60.4 (OCH<sub>3</sub>), 60.7 (OCH<sub>3</sub>), 60.7 (OCH<sub>3</sub>), 60.8  
673 (OCH<sub>3</sub>), 61.5(C6'<sub>Ac</sub>), 61.7 (C6<sub>Ac</sub>), 62.8 (OCH<sub>2</sub>-triazole), 67.8 (C4'<sub>Ac</sub>), 70.0 (C6<sub>Me</sub>),  
674 71.2 (C6'<sub>Me</sub>), 71.4 (C2<sub>Ac</sub> or C2'<sub>Ac</sub>), 71.6 (C2<sub>Ac</sub> or C2'<sub>Ac</sub>), 72.0 (C5<sub>Ac</sub>), 72.4 (C5'<sub>Ac</sub>),  
675 72.8 (C3<sub>Ac</sub> or C3'<sub>Ac</sub>), 72.9 (C3<sub>Ac</sub> or C3'<sub>Ac</sub>), 74.8 (C5'<sub>Me</sub>), 76.3(C4<sub>Ac</sub>), 77.9 (C4<sub>Me</sub>),  
676 79.3 (C4'<sub>Me</sub>), 82.1 (C2<sub>Me</sub>), 84.0 (C2'<sub>Me</sub>), 85.2 (C3<sub>Me</sub>), 87.0 (C3'<sub>Me</sub>), 87.3 (C1<sub>Me</sub>),  
677 99.6 (C1<sub>Ac</sub>), 100.7 (C1'<sub>Ac</sub>), 103.3 (C1'<sub>Me</sub>), 122.0 (triazole CH), 144.3 (O-CH<sub>2</sub>-C=),  
678 169.0, 169.3, 169.6, 169.7, 170.2, 170.5 (COCH<sub>3</sub>)

679 **1-[2,3,4,6-Tetra-*O*-methyl- $\beta$ -D-glucopyranosyl-(1 $\rightarrow$ 4)-2,3,6-tri-*O*-methyl- $\beta$ -**  
680 **D-glucopyranosyl]-4-[ $\beta$ -D-glucopyranosyl-(1 $\rightarrow$ 4)- $\beta$ -D-**  
681 **glucopyranosyloxymethyl]-1*H*-1,2,3-triazole (1a)**

682 Sodium methoxide (28%) in methanol (0.01 mL, 1.4 equiv.) was added at room  
683 temperature to a solution of 1-[2,3,4,6-tetra-*O*-methyl- $\beta$ -D-glucopyranosyl-  
684 (1 $\rightarrow$ 4)-2,3,6-tri-*O*-methyl- $\beta$ -D-glucopyranosyl]-4-[2,3,4,6-tetra-*O*-acetyl- $\beta$ -D-  
685 glucopyranosyl-(1 $\rightarrow$ 4)-2,3,6-tri-*O*-acetyl- $\beta$ -D-glucopyranosyloxymethyl]-1*H*-  
686 1,2,3-triazole (**4a**, 146 mg, 0.128 mmol) in MeOH (1 mL) and THF (1 mL). The  
687 mixture was stirred for 3 h at room temperature. The solution was neutralized with  
688 Amberlyst H<sup>+</sup>. The Amberlyst H<sup>+</sup> was removed by filtration and washed with  
689 MeOH. The combined filtrate and washings were concentrated to dryness to give  
690 1-[2,3,4,6-tetra-*O*-methyl- $\beta$ -D-glucopyranosyl-(1 $\rightarrow$ 4)-2,3,6-tri-*O*-methyl- $\beta$ -D-  
691 glucopyranosyl]-4-[ $\beta$ -D-glucopyranosyl-(1 $\rightarrow$ 4)- $\beta$ -D-glucopyranosyloxymethyl]-  
692 1*H*-1,2,3-triazole (**1a**, 108.3 mg, quantitative yield).

693 <sup>1</sup>H-NMR (500 MHz, D<sub>2</sub>O):  $\delta$  3.01 (t, 1H,  $J$ =9.5 Hz, H2'<sub>Me</sub>), 3.03 (s, 3H, OCH<sub>3</sub>),  
694 3.18 (t, 1H,  $J$ =10.0 Hz, H4'<sub>Me</sub>), 3.21 (H2<sub>OH</sub>), 3.21 (H2'<sub>OH</sub>), 3.25 (t, 1H,  $J$ =10.0 Hz,  
695 H3'<sub>Me</sub>), 3.25 (s, 3H, OCH<sub>3</sub>), 3.28 (H4'<sub>OH</sub>), 3.31 (s, 3H, OCH<sub>3</sub>), 3.33-3.38 (m, 1H,  
696 H5<sub>OH</sub>), 3.36 (t, 1H,  $J$ =9.0 Hz, H3'<sub>OH</sub>), 3.38 (H5'<sub>Me</sub>), 3.43 (s, 3H, OCH<sub>3</sub>), 3.49 (s,  
697 3H, OCH<sub>3</sub>), 3.5 (H3<sub>OH</sub>), 3.50-3.56 (H4<sub>OH</sub>), 3.52 (s, 6H, OCH<sub>3</sub>), 3.56-3.7 (H6<sub>Me</sub> and  
698 H6'<sub>Me</sub>), 3.58-3.86 (H6<sub>OH</sub> and H6'<sub>OH</sub>), 3.62 (H3<sub>Me</sub>), 3.73 (t, 1H,  $J$ =9.0 Hz, H2<sub>Me</sub>),  
699 3.79 (t, 1H,  $J$ =10.0 Hz, H4<sub>Me</sub>), 3.86 (m, 1H, H5<sub>Me</sub>), 4.33 (d, 1H,  $J$ =8.0 Hz, H1'<sub>Me</sub>),  
700 4.38 (d, 1H,  $J$ =8.5 Hz, H1'<sub>OH</sub>), 4.46 (d, 1H,  $J$ =7.5 Hz, H1<sub>OH</sub>), 4.81 (d, 1H,  $J$ =13.0  
701 Hz, OCH<sub>2</sub>-triazole), 4.90 (d, 1H,  $J$ =13.0 Hz, OCH<sub>2</sub>-triazole), 5.68 (d, 1H,  $J$ =9.0  
702 Hz, H1<sub>Me</sub>), 8.24 (s, 1H, triazole CH)

703  $^{13}\text{C}$ -NMR (125 MHz,  $\text{D}_2\text{O}$ ):  $\delta$  61.0 ( $\text{OCH}_3$ ), 61.1 ( $\text{OCH}_3$ ), 62.3 ( $\text{OCH}_3$ ), 62.6  
704 ( $\text{OCH}_3$ ), 62.6 ( $\text{C6}_{\text{OH}}$  or  $\text{C6}'_{\text{OH}}$ ), 62.7 ( $\text{OCH}_3$ ), 63.2 ( $\text{OCH}_3$ ), 63.2 ( $\text{C6}_{\text{OH}}$  or  $\text{C6}'_{\text{OH}}$ ),  
705 64.6 ( $\text{OCH}_2$ -triazole), 72.1 ( $\text{C4}'_{\text{OH}}$ ), 72.4 ( $\text{C6}_{\text{Me}}$  or  $\text{C6}'_{\text{Me}}$ ), 73.1 ( $\text{C6}_{\text{Me}}$  or  $\text{C6}'_{\text{Me}}$ ),  
706 75.4 ( $\text{C2}'_{\text{OH}}$ ), 75.8 ( $\text{C2}_{\text{OH}}$ ), 76.1 ( $\text{C3}'_{\text{OH}}$ ), 76.9 ( $\text{C3}_{\text{OH}}$ ), 77.4 ( $\text{C5}_{\text{OH}}$ ), 78.1 ( $\text{C5}_{\text{OH}}$  or  
707  $\text{C5}'_{\text{Me}}$ ), 78.6 ( $\text{C4}_{\text{Me}}$ ), 78.7 ( $\text{C5}_{\text{OH}}$  or  $\text{C5}'_{\text{Me}}$ ), 79.3 ( $\text{C5}_{\text{Me}}$ ), 81.1 ( $\text{C4}_{\text{OH}}$ ), 81.4 ( $\text{C4}'_{\text{Me}}$ ),  
708 83.9 ( $\text{C2}_{\text{Me}}$ ), 85.4 ( $\text{C2}'_{\text{Me}}$ ), 86.0 ( $\text{C3}_{\text{Me}}$ ), 87.6 ( $\text{C3}'_{\text{Me}}$ ), 88.9 ( $\text{C1}_{\text{Me}}$ ), 104.1 ( $\text{C1}_{\text{OH}}$ ),  
709 105.1 ( $\text{C1}'_{\text{Me}}$ ), 105.2 ( $\text{C1}'_{\text{OH}}$ ), 127.5 (triazole CH), 146.9 ( $\text{O-CH}_2\text{-C=}$ )

710 MALDI-TOF MS ( $m/z$ ): calcd for  $\text{C}_{34}\text{H}_{59}\text{N}_3\text{O}_{21}$ , 845.36; found,  $[\text{M}+\text{Na}]^+ =$   
711 868.586,  $[\text{M}+\text{K}]^+ = 884.580$

712

713 **1-(2,3,6-Tri-*O*-methyl-cellulosyl)-4-[2,3,4,6-tetra-*O*-acetyl- $\beta$ -D-**  
714 **glucopyranosyl-(1 $\rightarrow$ 4)-2,3,6-tri-*O*-acetyl- $\beta$ -D-glucopyranosyloxymethyl]-1*H*-**  
715 **1,2,3-triazole (4b)**

716 Compound **4b** was prepared according to our previous paper (Yamagami et al.  
717 2018). GPC analysis:  $M_n = 7.4 \times 10^3$ ,  $M_w / M_n = 1.4$ ,  $DP_n = 34.8$ .

718

719 **1-(2,3,6-Tri-*O*-methyl-cellulosyl)-4-[ $\beta$ -D-glucopyranosyl-(1 $\rightarrow$ 4)- $\beta$ -D-**  
720 **glucopyranosyloxymethyl]-1*H*-1,2,3-triazole (1b)**

721 Compound **1b** was prepared according to our previous paper (Yamagami et al.  
722 2018). GPC analysis:  $M_n = 6.8 \times 10^3$ ,  $M_w / M_n = 1.4$ ,  $DP_n = 33$ .

723

724 **1-[2,3,4,6-Tetra-*O*-methyl- $\beta$ -D-glucopyranosyl-(1 $\rightarrow$ 4)-2,3,6-tri-*O*-methyl- $\beta$ -**  
725 **D-glucopyranosyl]-4-(*N* $\alpha$ -Fmoc-*N* $\omega$ -Pbf-L-arginine-*N* $\omega$ -Pbf-L-arginine-*N*-**  
726 **methyl)-1*H*-1,2,3-triazole (5a)**

727 To a solution of 2,3,4,6-tetra-*O*-methyl- $\beta$ -D-glucopyranosyl-(1 $\rightarrow$ 4)-2,3,6-tri-*O*-  
728 methyl- $\beta$ -D-glucopyranosyl azide (**7a**, 25 mg, 0.054 mmol) and Fmoc-Arg(Pbf)-  
729 Arg(Pbf)-NH-CH<sub>2</sub>CCH (**9**, 59 mg, 0.054 mmol) in 3 mL of  
730 methanol/dichloromethane (1/4, v/v) were added CuBr (77 mg, 0.054 mmol, 10  
731 equiv.) and aqueous sodium ascorbate (213 mg/269  $\mu$ L). The reaction mixture  
732 was stirred under nitrogen at room temperature for 2 h. The mixture was purified  
733 by preparative TLC (eluent: 1:9 (v/v) methanol/dichloromethane) to give 1-  
734 [2,3,4,6-tetra-*O*-methyl- $\beta$ -D-glucopyranosyl-(1 $\rightarrow$ 4)-2,3,6-tri-*O*-methyl- $\beta$ -D-  
735 glucopyranosyl]-4-(*N* $\alpha$ -Fmoc-*N* $\omega$ -Pbf-L-arginine-*N* $\omega$ -Pbf-L-arginine-*N*-methyl)-  
736 1*H*-1,2,3-triazole (**5a**, 71 mg, 0.045 mmol, 85% yield).

737 <sup>1</sup>H-NMR (500 MHz, CDCl<sub>3</sub>):  $\delta$ : 1.44 (CH<sub>3</sub>, Pbf), 1.59 (H $\gamma$ ), 1.85 (H $\beta$ ), 2.06-  
738 2.09 (CH<sub>3</sub>, Pbf), 2.49-2.59 (CH<sub>3</sub>, Pbf), 2.92 (CH<sub>2</sub>, Pbf), 2.94 (CH<sub>2</sub>, Pbf), 2.92 (t,  
739 1H, *J*=9.0 Hz, H2'<sub>Me</sub>), 3.11 (OCH<sub>3</sub>), (3.12 (t, 1H, *J*=9.0 Hz, H3'<sub>Me</sub>), 3.15 (t, 1H,  
740 *J*=9.0 Hz, H4'<sub>Me</sub>), 3.21-3.25 (m, 1H, H5'<sub>Me</sub>), 3.22 (OCH<sub>3</sub>), 3.26 (H $\delta$ ), 3.40 (OCH<sub>3</sub>),  
741 3.35 (t, 1H, *J*=8.5 Hz, H3<sub>Me</sub>), 3.38 (OCH<sub>3</sub>), 3.52 (OCH<sub>3</sub>), 3.53 (OCH<sub>3</sub>), 3.59  
742 (OCH<sub>3</sub>), 3.62 (OCH<sub>3</sub>), 3.5-3.7 (H6'<sub>Me</sub>, H2<sub>Me</sub>, H5<sub>Me</sub>), 3.6-3.75 (2H, H6<sub>Me</sub>), 3.75 (t,  
743 1H, *J*=9.5 Hz, H4<sub>Me</sub>), 4.1-4.35 (broad s, H $\alpha$ ), 4.18-4.24 (1H, H (Fmoc)), 4.30  
744 (H1'<sub>Me</sub>), 4.32-4.36 (CH<sub>2</sub>, Fmoc), 4.43-4.60 (broad d, broad d, 2H, NH-CH<sub>2</sub>-  
745 triazole), 5.41 (H1<sub>Me</sub>), 5.60 (NH), 6.0-6.6 (NH), 7.2-7.8 (arom. H, Fmoc)

746 <sup>13</sup>C-NMR (125 MHz, CDCl<sub>3</sub>):  $\delta$  12.5 (CH<sub>3</sub>, Pbf), 17.9 (CH<sub>3</sub>, Pbf), 19.3 (CH<sub>3</sub>,  
747 Pbf), 25.6 (C $\gamma$ ), 28.6 (CH<sub>3</sub>, Pbf), 29.7 (C $\beta$ ), 40.8 (C $\delta$ ), 43.2 (CH<sub>2</sub>, Pbf), 47.0 (CH,  
748 Fmoc), 53.6 (C $\alpha$ ), 54.4 (C $\alpha$ ), 58.7, 59.3, 60.4, 60.6, 60.8 (OCH<sub>3</sub>), 67.3 (CH<sub>2</sub>,  
749 Fmoc), 70.1 (C6), 71.2 (C6'), 74.7 (C5'), 77.2 (C4), 77.4 (C5), 79.3 (C4'), 81.8  
750 (C2), 84.0 (C2'), 85.2 (C3), 86.4 (CH, Fmoc), 86.4 (CH, Fmoc), 86.9 (C3'), 87.0  
751 (C1), 103.3 (C1'), 117.6 (arom. Pbf), 119.9 (arom. Fmoc), 120.0, 122.5 (triazole)

752 CH), 124.6 (arom. Pbf), 124.9 (arom. Fmoc), 125.2 (arom. Fmoc), 127.1 (arom.  
753 Fmoc), 127.6 (arom. Fmoc), 132.3 (arom. Pbf), 132.7 (arom. Pbf), 138.3 (arom.  
754 Pbf), 141.1 (arom. Fmoc), 143.7 (arom. Fmoc), 144.5 (O-CH<sub>2</sub>-C=), 156.4 (arom.  
755 Pbf), 158.7 (-O-C arom. Pbf), 172.2 (Arg, C $\alpha$ -CO-NH-), 173.5 (Arg, C $\alpha$ -CO-NH)  
756 MALDI-TOF MS (*m/z*): calcd for C<sub>75</sub>H<sub>108</sub>N<sub>12</sub>O<sub>20</sub>S<sub>2</sub>, 1560.72; found, [M+H]<sup>+</sup> =  
757 1559.755, [M+Na]<sup>+</sup> = 1581.722, [M+K]<sup>+</sup> = 1597.671  
758

759 **1-[2,3,4,6-Tetra-*O*-methyl- $\beta$ -D-glucopyranosyl-(1 $\rightarrow$ 4)-2,3,6-tri-*O*-methyl- $\beta$ -**  
760 **D-glucopyranosyl]-4-(Arg-Arg-NH-CH<sub>2</sub>)-1*H*-1,2,3-triazole (2a)**  
761 1-[2,3,4,6-Tetra-*O*-methyl- $\beta$ -D-glucopyranosyl-(1 $\rightarrow$ 4)-2,3,6-tri-*O*-methyl- $\beta$ -D-  
762 glucopyranosyl]-4-(*N* $\alpha$ -Fmoc-*N* $\omega$ -Pbf-L-arginine-*N* $\omega$ -Pbf-L-arginine-*N*-methyl)-  
763 1*H*-1,2,3-triazole (**5a**, 61 mg, 0.039 mmol) was dissolved in  
764 piperidine/dichloromethane (1/1, v/v, 1 mL). The reaction mixture was stirred  
765 under nitrogen at room temperature for 1 h and then concentrated to dryness. The  
766 crude product was purified by preparative TLC (eluent: 15:85 (v/v)  
767 methanol/dichloromethane) to give 1-[2,3,4,6-tetra-*O*-methyl- $\beta$ -D-  
768 glucopyranosyl-(1 $\rightarrow$ 4)-2,3,6-tri-*O*-methyl- $\beta$ -D-glucopyranosyl]-4-(*N* $\omega$ -Pbf-L-  
769 arginine-*N* $\omega$ -Pbf-L-arginine-*N*-methyl)-1*H*-1,2,3-triazole (34 mg, 0.025 mmol,  
770 65% yield; MALDI-TOF MS (*m/z*): calcd for C<sub>60</sub>H<sub>96</sub>N<sub>12</sub>O<sub>18</sub>S<sub>2</sub>, 1336.64; found,  
771 [M+Na]<sup>+</sup> = 1359.5).

772 1-[2,3,4,6-Tetra-*O*-methyl- $\beta$ -D-glucopyranosyl-(1 $\rightarrow$ 4)-2,3,6-tri-*O*-methyl- $\beta$ -D-  
773 glucopyranosyl]-4-(*N* $\omega$ -Pbf-L-arginine-*N* $\omega$ -Pbf-L-arginine-*N*-methyl)-1*H*-1,2,3-  
774 triazole (31 mg, 0.023 mmol) was dissolved in TFA/distilled water (8/2, v/v, 1.0  
775 mL) and stirred under nitrogen at 37 °C for 4 h. The reaction mixture was  
776 concentrated to dryness and the crude product was purified by gel-filtration

777 column chromatography (LH-20, eluent: methanol) to give 1-[2,3,4,6-tetra-*O*-  
778 methyl- $\beta$ -D-glucopyranosyl-(1 $\rightarrow$ 4)-2,3,6-tri-*O*-methyl- $\beta$ -D-glucopyranosyl]-4-  
779 (Arg-Arg-NH-CH<sub>2</sub>)-1*H*-1,2,3-triazole (**2a**, 10 mg, 0.012 mmol, 52% yield).

780 <sup>1</sup>H-NMR (500 MHz, D<sub>2</sub>O):  $\delta$  1.5-1.7 (m, 4H, H $\gamma$  and H $\gamma'$ ), 1.73-1.83 (m, 2H,  
781 H $\beta$ ), 1.85-1.95 (m, 2H, H $\beta'$ ), 3.09 (s, 3H, OCH<sub>3</sub>), 3.12 (t, *J*=9.5 Hz, H2'), 3.12-  
782 3.25 (m, 4H, H $\delta$  and H $\delta'$ ), 3.29 (t, *J*=9.0 Hz, H4'), 3.36 (t, *J*=9.0 Hz, H3'), 1H,  
783 3.36 (s, 3H, OCH<sub>3</sub>), 3.42 (s, 3H, OCH<sub>3</sub>), 3.46 (m, 1H, H5'), 3.54 (s, 3H, OCH<sub>3</sub>),  
784 3.60 (s, 3H, OCH<sub>3</sub>), 3.63 (s, 3H, OCH<sub>3</sub>), 3.63 (s, 3H, OCH<sub>3</sub>), 3.67-3.75 (2H, H6'),  
785 3.70 (t, 1H, *J*=9.5 Hz, H3), 3.72-3.78 (2H, H6), 3.81 (t, 1H, *J*=9.0 Hz, H2), 3.89 (t,  
786 1H, *J*=9.0 Hz, H4), 3.97 (m, 1H, H5), 4.04 (broad s, 1H, H $\alpha'$ ), 4.30 (t, 1H, *J*=6.5  
787 Hz, H $\alpha$  (near sugar residue)), 4.44 (d, 1H, *J*=8.0 Hz, H1'), 4.44 (d, 1H, *J*=14.5 Hz,  
788 NHCH<sub>2</sub>-triazole), 4.57 (d, 1H, *J*=15.5 Hz, OCH<sub>2</sub>-triazole), 5.75 (d, 1H, *J*=9.5 Hz,  
789 H1), 8.19 (s, 1H, CH, triazole)

790 <sup>13</sup>C-NMR (125 MHz, D<sub>2</sub>O):  $\delta$  26.0 (C $\gamma'$ ), 26.9 (C $\gamma$ ), 30.6 (C $\beta$  or C $\beta'$ ), 30.8 (C $\beta$   
791 or C $\beta'$ ), 36.8 (NHCH<sub>2</sub>-triazole), 43.0 (C $\delta$  or C $\delta'$ ), 43.1 (C $\delta$  or C $\delta'$ ), 51.5 (C $\alpha'$ ),  
792 56.6 (C $\alpha$  (near sugar residue)), 61.0 (OCH<sub>3</sub>), 61.1 (OCH<sub>3</sub>), 62.4 (OCH<sub>3</sub>), 62.5  
793 (OCH<sub>3</sub>), 62.6 (OCH<sub>3</sub>), 62.7 (OCH<sub>3</sub>), 63.2 (OCH<sub>3</sub>), 72.5 (C6), 73.1 (C6'), 76.1  
794 (C5'), 78.7 (C4), 79.3 (C5), 81.4 (C4'), 84.0 (C2), 85.4 (C2'), 86.0 (C3), 87.8 (C3'),  
795 88.9 (C1), 105.1 (C1'), 126.2 (CH of triazole), 147.5 (quaternary C of triazole).  
796 159.4 (quaternary C of guanidino group of arginine), 159.4 (quaternary C of  
797 guanidino group of arginine), 175.8 (C $\alpha$ -CO-NH-), 175.9 (C $\alpha'$ -CO-NH-)

798 MALDI-TOF MS (*m/z*): calcd for C<sub>34</sub>H<sub>64</sub>N<sub>12</sub>O<sub>12</sub>, 832.48; found, [M+H]<sup>+</sup> =  
799 833.63  
800

801 **1-[2,3,4,6-Tetra-*O*-methyl- $\beta$ -D-glucopyranosyl-(1 $\rightarrow$ 4)-2,3,6-tri-*O*-methyl- $\beta$ -**  
802 **D-glucopyranosyl]-4-[Fmoc-Glu(*O**t*-Bu)-Glu(*O**t*-Bu)-*N*-methyl]-1*H*-1,2,3-**  
803 **triazole (6a)**

804 To a solution of 2,3,4,6-tetra-*O*-methyl- $\beta$ -D-glucopyranosyl-(1 $\rightarrow$ 4)-2,3,6-tri-*O*-  
805 methyl- $\beta$ -D-glucopyranosyl azide (**7a**, 25 mg, 0.054 mmol) and Fmoc-  
806 Glu(*O**t*Bu)-Glu(*O**t*Bu)-NH-CH<sub>2</sub>CCH (**10**, 35 mg, 0.054 mmol) in 3 mL of  
807 methanol/dichloromethane (1/4, v/v) were added CuBr (77 mg, 0.054 mmol, 10  
808 equiv.) and aqueous sodium ascorbate (213 mg/269  $\mu$ L). The reaction mixture  
809 was stirred under nitrogen at room temperature for 2 h, after which it was purified  
810 by PTLC (eluent: 1:9 (v/v) methanol/dichloromethane) to give 1-(2,3,4,6-tetra-*O*-  
811 methyl- $\beta$ -D-glucopyranosyl-(1 $\rightarrow$ 4)-2,3,6-tri-*O*-methyl- $\beta$ -D-glucopyranosyl)-4-  
812 [*N* $\alpha$ -Fmoc-Glu(*O**t*-Bu)-Glu(*O**t*-Bu)-*N*-methyl]-1*H*-1,2,3-triazole (52 mg, 0.047  
813 mmol, 87% yield).

814 <sup>1</sup>H-NMR (500 MHz, CDCl<sub>3</sub>):  $\delta$ : 1.42 (s, 9H, CH<sub>3</sub> (*t*Bu)), 1.46 (s, 9H, CH<sub>3</sub> (*t*Bu)),  
815 1.90-2.02 (m, 2H, H $\beta$ ), 2.02-2.20 (m, 2H, H $\beta$ ), 2.26-2.48 (m, 4H, H $\gamma$ ), 2.96 (t, 1H,  
816  $J$ =8.5 Hz, H2'<sub>Me</sub>), 3.14 (t, 1H,  $J$ =9.0 Hz, H3'<sub>Me</sub>), 3.15 (s, 3H, OCH<sub>3</sub>), 3.20 (t, 1H,  
817  $J$ =8.5 Hz, H4'<sub>Me</sub>), 3.23-3.28 (H5'<sub>Me</sub>), 3.30 (s, 3H, OCH<sub>3</sub>), 3.39 (t, 1H,  $J$ =8.5 Hz,  
818 H3<sub>Me</sub>), 3.42 (s, 3H, OCH<sub>3</sub>), 3.54 (s, 3H, OCH<sub>3</sub>), 3.56 (s, 3H, OCH<sub>3</sub>), 3.62 (s, 3H,  
819 OCH<sub>3</sub>), 3.63 (s, 3H, OCH<sub>3</sub>), 3.54-3.58 (m, H5<sub>Me</sub>), 3.58-3.67 (3H, H6<sub>Me</sub>, H6'<sub>Me</sub>),  
820 3.64 (t, 1H,  $J$ =9.0 Hz, H2<sub>Me</sub>), 3.6-3.75 (dd, 1H,  $J$ =4.5 Hz,  $J$ =11.0 Hz, H6<sub>Me</sub>), 3.79  
821 (t, 1H,  $J$ =9.5 Hz, H4<sub>Me</sub>), 4.12 (m, 1H, H $\alpha$ ), 4.20 (t, 1H,  $J$ =4.5 Hz, CH (Fmoc)),  
822 4.32 (d, 1H,  $J$ =8.0 Hz, H1<sub>Me</sub>), 4.35 (broad d, 2H,  $J$ =7.0 Hz, CH<sub>2</sub> (Fmoc)), 4.43 (m,  
823 1H, H $\alpha$ ), 4.54 (broad d,  $J$ =5.5 Hz, NH-CH<sub>2</sub>-triazole), 5.39 (d, 1H,  $J$ =9.0 Hz, H1<sub>Me</sub>),  
824 6.07 (d,  $J$ =6.0 Hz, NH-C $\alpha$ ), 7.28-7.78 (8H, arom. Fmoc), 7.74 (broad s, triazole  
825 H)



826  $^{13}\text{C}$ -NMR (125 MHz,  $\text{CDCl}_3$ ):  $\delta$  27.0 (triazole- $\text{CH}_2$ -NH- $\underline{\text{C}\alpha}$ - $\underline{\text{C}\beta}$ -), 27.3 ( $\underline{\text{C}\beta}$ - $\underline{\text{C}\alpha}$ -  
827 NH-Fmoc), 28.0 ( $\text{CH}_3$  (tBu)), 28.0 ( $\text{CH}_3$  (tBu)), 31.8 (triazole- $\text{CH}_2$ -NH- $\underline{\text{C}\alpha}$ - $\underline{\text{C}\beta}$ -  
828  $\underline{\text{C}\gamma}$ ), 31.8 ( $\underline{\text{C}\gamma}$ - $\underline{\text{C}\beta}$ - $\underline{\text{C}\alpha}$ -NH-Fmoc), 35.1 (triazole- $\underline{\text{CH}_2}$ -NH-), 47.1 ( $\underline{\text{CH}}$ , Fmoc),  
829 53.0 (triazole- $\text{CH}_2$ -NH-CO- $\underline{\text{C}\alpha}$ -NH-), 55.3 (-CO- $\underline{\text{C}\alpha}$ -NH-Fmoc), 59.0 ( $\text{OCH}_3$ ),  
830 59.3 ( $\text{OCH}_3$ ), 60.3 ( $\text{OCH}_3$ ), 60.3 ( $\text{OCH}_3$ ), 60.6 ( $\text{OCH}_3$ ), 60.7 ( $\text{OCH}_3$ ), 60.8 ( $\text{OCH}_3$ ),  
831 67.1 ( $\underline{\text{CH}_2}$ , Fmoc), 70.0 (C6), 71.1 (C6'), 74.7 (C5'), 77.1 (C4), 77.8 (C5), 79.3  
832 (C4'), 81.1 ( $\underline{\text{C}}(\text{CH}_3)_3$ ), 81.3 ( $\underline{\text{C}}(\text{CH}_3)_3$ ), 81.9 (C2), 84.0 (C2'), 85.3 (C3), 86.9 (C3'),  
833 87.2 (C1), 103.2 (C1'), 119.9 (arom. Fmoc), 121.6 (triazole  $\underline{\text{CH}}$ ), 125.2 (arom.  
834 Fmoc), 127.1 (arom. Fmoc), 127.1 (arom. Fmoc), 127.7 (arom. Fmoc), 141.2  
835 (arom. Fmoc), 141.3 (arom. Fmoc), 143.7 (arom. Fmoc), 143.9 (arom. Fmoc),  
836 144.8 ( $\text{O}-\text{CH}_2-\text{C}=\text{O}$ ), 156.6 (CO Fmoc), 171.0 (Glu, triazole- $\text{CH}_2$ -NH- $\underline{\text{CO}}$ - $\underline{\text{C}\alpha}$ -NH-),  
837 171.6 (Glu, - $\underline{\text{CO}}$ - $\underline{\text{C}\alpha}$ -NH-Fmoc), 173.1 (Glu, C $\delta$ ), 173.1 (Glu, C $\delta$ )

838 MALDI-TOF MS ( $m/z$ ): calcd for  $\text{C}_{55}\text{H}_{80}\text{N}_6\text{O}_{18}$ , 1112.55; found,  $[\text{M}+\text{Na}]^+ =$   
839 1135.615,  $[\text{M}+\text{K}]^+ = 1151.583$

840

841 **1-[2,3,4,6-Tetra-*O*-methyl- $\beta$ -D-glucopyranosyl-(1 $\rightarrow$ 4)-2,3,6-tri-*O*-methyl- $\beta$ -**  
842 **D-glucopyranosyl]-4-(Glu-Glu-NH- $\text{CH}_2$ )-1*H*-1,2,3-triazole (3a)**

843 1-[2,3,4,6-Tetra-*O*-methyl- $\beta$ -D-glucopyranosyl-(1 $\rightarrow$ 4)-2,3,6-tri-*O*-methyl- $\beta$ -D-  
844 glucopyranosyl]-4-[*N* $\alpha$ -Fmoc-Glu(*O**t*-Bu)-Glu(*O**t*-Bu)-*N*-methyl]-1*H*-1,2,3-  
845 triazole (**6a**, 46 mg, 0.034 mmol) was dissolved in piperidine/dichloromethane  
846 (1/1, v/v, 1 mL). The reaction mixture was stirred under nitrogen at room  
847 temperature for 1 h, and then concentrated to dryness. The crude product was  
848 purified by PTLC (eluent: methanol/dichloromethane (15/85, v/v)) to give 1-  
849 [2,3,4,6-tetra-*O*-methyl- $\beta$ -D-glucopyranosyl-(1 $\rightarrow$ 4)-2,3,6-tri-*O*-methyl- $\beta$ -D-

850 glucopyranosyl]-4-[Glu(*O**t*-Bu)-Glu(*O**t*-Bu)-*N*-methyl]-1*H*-1,2,3-triazole (24 mg,  
851 0.016 mmol, 47% yield).

852 1-[2,3,4,6-Tetra-*O*-methyl- $\beta$ -D-glucopyranosyl-(1 $\rightarrow$ 4)-2,3,6-tri-*O*-methyl- $\beta$ -D-  
853 glucopyranosyl]-4-(Glu(*O**t*-Bu)-Glu(*O**t*-Bu)-*N*-methyl)-1*H*-1,2,3-triazole (66 mg,  
854 0.079 mmol) was dissolved in TFA/dichloromethane (9/1, v/v, 1 mL) and stirred  
855 under nitrogen at room temperature for 4 h. The crude product was purified by  
856 gel-filtration chromatography (LH-20, eluent: methanol) to give 1-[2,3,4,6-tetra-  
857 *O*-methyl- $\beta$ -D-glucopyranosyl-(1 $\rightarrow$ 4)-2,3,6-tri-*O*-methyl- $\beta$ -D-glucopyranosyl]-4-  
858 (Glu-Glu-*N*-methyl)-1*H*-1,2,3-triazole (**3a**, 36 mg, 0.046 mmol, 58% yield).

859 <sup>1</sup>H-NMR (500 MHz, D<sub>2</sub>O):  $\delta$  1.9-2.1 (m, 2H, H $\beta$ ), 2.2-2.3 (m, 2H, H $\beta$ ), 2.3-2.6  
860 (m, 4H, H $\gamma$ ), 3.12 (t, 1H,  $J=8.5$  Hz, H2'<sub>Me</sub>), 3.29 (t, 1H,  $J=9.5$  Hz, H4'<sub>Me</sub>), 3.36 (t,  
861 1H,  $J=8.5$  Hz, H3'<sub>Me</sub>), 3.36 (s, 3H, OCH<sub>3</sub>), 3.42 (s, 3H, OCH<sub>3</sub>), 3.43-3.48 (H5'<sub>Me</sub>),  
862 3.54 (s, 3H, OCH<sub>3</sub>), 3.60 (s, 3H, OCH<sub>3</sub>), 3.62 (s, 3H, OCH<sub>3</sub>), 3.63 (s, 6H, OCH<sub>3</sub>),  
863 3.7 (H3<sub>Me</sub>), 3.80 (t, 1H,  $J=9.5$  Hz, H2<sub>Me</sub>), 3.89 (t, 1H,  $J=9.5$  Hz, H4<sub>Me</sub>), 3.93-3.98  
864 (m, 1H, H5<sub>Me</sub>), 3.65-3.83 (H6'<sub>Me</sub>, H6<sub>Me</sub>), 3.79 (t, 1H,  $J=9.5$  Hz, H4<sub>Me</sub>), 3.86 (m, 1H,  
865 H5<sub>Me</sub>), 4.2-4.5 (broad s, 1H, H $\alpha$ ), 4.34 (d, 1H,  $J=8.0$  Hz, H1'<sub>Me</sub>), 4.4-4.61 (NH-  
866 CH<sub>2</sub>-triazole), 5.75 (broad d, 1H,  $J=7.0$  Hz, H1<sub>Me</sub>), 8.24 (broad s, triazole *CH*)

867 <sup>13</sup>C-NMR (125 MHz, D<sub>2</sub>O):  $\delta$  27.9 (C $\beta$ '), 29.0 (C $\beta$ ), 31.9 (C $\gamma$  and C $\gamma'$ ), 37.1  
868 (NHCH<sub>2</sub>-triazole), 56.1 (C $\alpha$  (near sugar residue)), 59.4 (C $\alpha'$ ), 61.1 (OCH<sub>3</sub>), 61.2  
869 (OCH<sub>3</sub>), 62.2 (OCH<sub>3</sub>), 62.5 (OCH<sub>3</sub>), 62.6 (OCH<sub>3</sub>), 62.7 (OCH<sub>3</sub>), 63.2 (OCH<sub>3</sub>),  
870 72.5 (C6 or C6'), 73.1 (C6 or C6'), 76.1 (C5'), 78.7 (C4), 79.4 (C5), 81.5 (C4'),  
871 84.0 (C2), 85.5 (C2'), 86.0 (C3), 87.8 (C3'), 89.1 (C1), 105.2 (C1'), 126.6 (CH of  
872 triazole), 177.6 (C $\alpha$ -CO-NH-, and C $\alpha'$ -CO-NH-), 184.9 (C $\gamma$ -(CO)OH, C $\gamma'$ -  
873 (CO)OH)

874 MALDI-TOF MS ( $m/z$ ): calcd for  $C_{32}H_{54}N_6O_{16}$ , 778.36; found,  $[M+H]^+ =$   
875 779.518,  $[M+Na]^+ = 801.530$ ,  $[M+K]^+ = 817.504$

876

877 **1-(Tri-*O*-methylcellulosyl)-4-(*N* $\alpha$ -Fmoc-*N* $\omega$ -Pbf-L-arginine-*N* $\omega$ -Pbf-L-**  
878 **arginine-*N*-methyl)-1*H*-1,2,3-triazole (**5b**)**

879 Sodium ascorbate (227 mg/287  $\mu$ L, 1.15 mmol, 20 equiv., 4 M in  $H_2O$ ) and  
880  $CuSO_4 \cdot 5H_2O$  (143 mg, MW = 249.69, 0.573 mmol, 10 equiv.) were added to a  
881 solution of 2-propynyl *N* $\alpha$ -Fmoc-*N* $\omega$ -Pbf-L-arginine-*N* $\omega$ -Pbf-L-arginine-*N*-  
882 propargylamide (**9**, 100 mg, MW = 788.8, 0.127 mmol, 2.2 equiv.) and tri-*O*-  
883 methylcellulosyl azide (**7b**, 419 mg,  $M_n = 7.34 \times 10^3$ ,  $DP_n = 35.8$ , 0.0571 mmol,  
884 1.0 equiv.) in methanol/dichloromethane (1/4, v/v, 10 mL). The reaction mixture  
885 was stirred at room temperature for 14 h under nitrogen, after which it was  
886 concentrated and passed through a silica-gel chromatography column (eluent:  
887 20% MeOH/ $CH_2Cl_2$ ) to give the crude product. The crude product was purified by  
888 gel-filtration column chromatography (LH-60, eluent: 20% MeOH/ $CH_2Cl_2$ ) to  
889 give 1-(tri-*O*-methylcellulosyl)-4-(*N* $\alpha$ -Fmoc-*N* $\omega$ -Pbf-L-arginine-*N* $\omega$ -Pbf-L-  
890 arginine-*N*-methyl)-1*H*-1,2,3-triazole (**5b**, 420 mg, quantitative yield; GPC  
891 analysis:  $M_n = 5.6 \times 10^3$ ,  $M_w / M_n = 1.8$ ).

892  $^1H$ -NMR (500 MHz,  $CDCl_3$ ):  $\delta$ : 1.44 ( $CH_3$ , Pbf), 2.07 ( $CH_3$ , Pbf), 2.47-2.56  
893 ( $CH_3$ , Pbf), 2.92 ( $CH_2$ , Pbf), 2.96 (t,  $J=8.5$  Hz,  $H_{2Me}$  (internal)), 3.21 (t, 1H,  $J=9.0$   
894 Hz,  $H_{3Me}$  (internal)), 3.29 (m,  $J=9.0$  Hz,  $H_{5Me}$  (internal)), 3.39 (s,  $OCH_3$ ), 3.54 (s,  
895  $OCH_3$ ), 3.58 (s,  $OCH_3$ ), 3.69 (t,  $J=9.0$ ,  $H_{4Me}$  (internal)), 3.6-3.73 (m,  $H_{6Me}$   
896 (internal)), 3.77 (m,  $H_{6Me}$  (internal)), 4.34 (d,  $J=8.0$  Hz,  $H_{1Me}$  (internal)), 6.12  
897 ( $H_{1\alpha Me}$ ), 6.1-6.7, 7.24 (Fmoc), 7.35 (Fmoc), 7.57 (Fmoc), 7.62 (d,  $J = 7.0$  Hz,  
898 Fmoc), 7.82.

899  $^{13}\text{C}$ -NMR (125 MHz,  $\text{CDCl}_3$ ):  $\delta$  12.5 ( $\text{CH}_3$ , Pbf), 17.9 ( $\text{CH}_3$ , Pbf), 19.3 ( $\text{CH}_3$ ,  
900 Pbf), 25.5 ( $\text{C}\gamma$ ), 28.6 ( $\text{CH}_3$ , Pbf), 40.9 ( $\text{C}\delta$ ), 43.2 ( $\text{CH}_2$ , Pbf), 47.0 ( $\text{CH}$ , Fmoc),  
901 59.1 ( $\text{OCH}_3$ ), 60.3 ( $\text{OCH}_3$ ), 60.5 ( $\text{OCH}_3$ ), 67.3 ( $\text{CH}_2$ , Fmoc), 70.3 ( $\text{C}_6$ ), 74.8 ( $\text{C}_5$ ),  
902 77.4 ( $\text{C}_4$ ), 83.5 ( $\text{C}_2$ ), 85.0 ( $\text{C}_3$ ), 86.4 ( $\text{CH}$ , Fmoc), 103.1 ( $\text{C}_1$ ), 117.6 (arom. Pbf),  
903 119.9 (arom. Fmoc), 124.7 (arom. Pbf), 125.2 (arom. Fmoc), 127.1 (arom. Fmoc),  
904 127.7 (arom. Fmoc), 132.3 (arom. Pbf), 132.7 (arom. Pbf), 138.3 (arom. Pbf),  
905 141.1 (arom. Fmoc), 143.7 (arom. Fmoc), 156.4 (arom. Pbf), 158.8 ( $-\text{O}-\text{C}$  arom.  
906 Pbf)

907 FT-IR (KBr): 3442, 2930, 2836, 1722, 1663, 1622, 1551, 1454, 1375, 1310,  
908 1125, 1184, 951, 853, 812, 785, 761, 741 (Fmoc), 700, 662, 567 (Pbf,  $-\text{SO}_2\text{NH}-$ )  
909  $\text{cm}^{-1}$

910

911 **1-(Tri-*O*-methylcellulosyl)-4-(L-arginine-L-arginine-*N*-methyl)-1*H*-1,2,3-**  
912 **triazole (2b)**

913 1-(Tri-*O*-methylcellulosyl)-4-( $N\alpha$ -Fmoc- $N\omega$ -Pbf-L-arginine- $N\omega$ -Pbf-L-  
914 arginine-*N*-methyl)-1*H*-1,2,3-triazole (**5b**, 293 mg) was dissolved in  
915 piperidine/dichloromethane (1/1, v/v, 4 mL). The reaction mixture was stirred at  
916 room temperature for 4 h under nitrogen, after which it was concentrated and  
917 purified by gel-filtration column chromatography (LH-60, eluent: 20%  
918 MeOH/ $\text{CH}_2\text{Cl}_2$ ) to give 1-(tri-*O*-methylcellulosyl)-4-( $N\omega$ -Pbf-L-arginine- $N\omega$ -Pbf-  
919 L-arginine-*N*-methyl)-1*H*-1,2,3-triazole (260 mg, 89% yield; GPC analysis:  $M_n$  =  
920  $6.7 \times 10^3$ ,  $M_w / M_n = 1.7$ ).

921 1-(Tri-*O*-methylcellulosyl)-4-( $N\omega$ -Pbf-L-arginine- $N\omega$ -Pbf-L-arginine-*N*-  
922 methyl)-1*H*-1,2,3-triazole (244 mg) was dissolved in trifluoroacetic acid/distilled  
923 water (1/4, v/v, 2 mL) and stirred at 37 °C for 4 h under nitrogen. The mixture

924 was concentrated, purified by gel-filtration column chromatography (LH-60,  
925 eluent: 20% MeOH/CH<sub>2</sub>Cl<sub>2</sub>), and further purified by PTLC (eluent: 10%  
926 MeOH/CH<sub>2</sub>Cl<sub>2</sub>). The purified 1-(tri-*O*-methyl-cellulosyl)-4-(L-arginine-L-  
927 arginine-*N*-methyl)-1*H*-1,2,3-triazole was dispersed in water. Water-soluble  
928 component was collected by removal of the water-insoluble component by  
929 filtration through cotton wool, which was then concentrated to give 1-(tri-*O*-  
930 methylcellulosyl)-4-(L-arginine-L-arginine-*N*-methyl)-1*H*-1,2,3-triazole (**2b**, 186  
931 mg, 76% yield, GPC analysis:  $M_n = 6.0 \times 10^3$ ,  $M_w / M_n = 1.6$ ).

932 <sup>1</sup>H-NMR (500 MHz, D<sub>2</sub>O): δ 1.5-2.0 (m, H<sub>γ</sub> and H<sub>γ'</sub>, H<sub>β</sub>, H<sub>β'</sub>), 3.13 (t,  $J = 8.5$   
933 Hz, H<sub>2Me</sub>), 3.40 (s, OMe), 3.45 (t,  $J = 9.5$  Hz, H<sub>3Me</sub>), 3.56 (s, OMe), 3.58 (s, OMe),  
934 3.55-3.60 (H<sub>5Me</sub>), 3.68-3.80 (H<sub>4Me</sub>, H<sub>6Me</sub>), 4.42 (d,  $J = 7.5$  Hz, H<sub>1Me</sub>), 4.65 (d,  $J =$   
935 8.0 Hz), 4.99 (d,  $J = 3.5$  Hz), 5.40 (d,  $J = 3.5$  Hz), 5.62 (broad s), 8.42 (s, CH,  
936 triazole)

937 FT-IR (KBr): 3446, 2922, 2836, 1624, 1456, 1375, 1314, 1125, 1078, 947, 768,  
938 702, 662, 606, 581, 538, 488 cm<sup>-1</sup>

940 **1-(Tri-*O*-methyl-cellulosyl)-4-[Fmoc-Glu(*O**t*-Bu)-Glu(*O**t*-Bu)-*N*-methyl]-**  
941 **1*H*-1,2,3-triazole (6b)**

942 Sodium ascorbate (109 mg/137 μL, 0.55 mmol, 20 equiv., 4 M in H<sub>2</sub>O) and  
943 CuSO<sub>4</sub>·5H<sub>2</sub>O (68 mg, MW = 249.69, 0.27 mmol, 10 equiv.) were added to a  
944 solution of *N*α-Fmoc-Glu(*O**t*-Bu)-Glu(*O**t*-Bu)-*N*-propargylamide (**10**, 53 mg,  
945 MW = 647.77, 0.082 mmol, 3.0 equiv.) and tri-*O*-methylcellulosyl azide (**7b**, 200  
946 mg,  $M_n = 7.34 \times 10^3$ ,  $DP_n = 35.8$ , 0.027 mmol, 1.0 equiv.) in  
947 methanol/dichloromethane (1/4, v/v, 5 mL). The reaction mixture was stirred at  
948 room temperature for 14 h under nitrogen, after which it was concentrated and

949 passed through a silica-gel chromatography column (eluent: 20% MeOH/CH<sub>2</sub>Cl<sub>2</sub>).  
950 The crude product was purified by gel-filtration column chromatography (LH-60,  
951 eluent: 20% MeOH/CH<sub>2</sub>Cl<sub>2</sub>), and then by PTLC (eluent: 10% MeOH/CH<sub>2</sub>Cl<sub>2</sub>) to  
952 give 1-(tri-*O*-methylcellulosyl)-4-[Fmoc-Glu(*O**t*-Bu)-Glu(*O**t*-Bu)-*N*-methyl]-1*H*-  
953 1,2,3-triazole (186 mg, 93% yield, GPC analysis:  $M_n = 7.4 \times 10^3$ ,  $M_w / M_n = 1.6$ ).

954 <sup>1</sup>H-NMR (500 MHz, CDCl<sub>3</sub>): δ 1.43 (s, CH<sub>3</sub> (*t*Bu)), 1.47 (s, CH<sub>3</sub> (*t*Bu)), 2.0-2.2  
955 (m, 4H, Hβ), 2.25-2.450 (m, 4H, Hγ), 2.96 (t, *J* = 8.5 Hz, H2<sub>Me</sub>), 3.22 (t, *J* = 9.0 Hz,  
956 H3<sub>Me</sub>), 3.29 (m, H5<sub>Me</sub>), 3.39 (s, OMe), 3.54 (s, OMe), 3.59 (s, OMe), 3.64-3.74  
957 (H4<sub>Me</sub>), 3.64-3.82 (H6<sub>Me</sub>), 4.1-4.2 (1H, Hα), 4.25-4.35 (2H, CH<sub>2</sub> (Fmoc)), 4.35 (d,  
958 *J* = 7.5 Hz, H1<sub>Me</sub>), 7.32 (t, *J* = 7.5 Hz, arom., Fmoc), 7.40 (t, *J* = 7.5 Hz, arom.,  
959 Fmoc), 7.62 (broad d, *J* = 7.0 Hz, arom., Fmoc), 7.76 (d, *J* = 7.5 Hz, arom., Fmoc)

960 <sup>13</sup>C-NMR (125 MHz, CDCl<sub>3</sub>): δ 28.0 (CH<sub>3</sub> (*t*Bu)), 28.0 (CH<sub>3</sub> (*t*Bu)), 31.9  
961 (triazole-CH<sub>2</sub>-NH-Cα-Cβ-Cγ), 35.2 (triazole-CH<sub>2</sub>-NH-), 47.1 (CH, Fmoc), 59.1  
962 (OCH<sub>3</sub>), 59.6, 60.1, 60.3 (OCH<sub>3</sub>), 60.4, 60.5 (OCH<sub>3</sub>), 60.8, 67.2 (CH<sub>2</sub>, Fmoc),  
963 70.3 (C6), 72.2, 73.2, 73.2, 74.9 (C5), 77.4 (C4), 81.2 (C(CH<sub>3</sub>)<sub>3</sub>), 83.5 (C2), 85.0  
964 (C3), 86.1, 103.1 (C1), 120.0 (arom. Fmoc), 125.1 (arom. Fmoc), 127.1 (arom.  
965 Fmoc), 127.7 (arom. Fmoc), 141.3 (arom. Fmoc), 143.8 (arom. Fmoc), 144.4  
966 (arom. Fmoc)

967 FT-IR (KBr): 3430, 2932, 2904, 2836, 1728, 1672, 1514 (*t*Bu), 1454, 1373,  
968 1312, 1125, 1084, 1059, 951, 889, 851, 762, 743 (Fmoc), 704, 656, 615, 577 cm<sup>-1</sup>  
969

970 **1-(Tri-*O*-methyl-cellulosyl)-4-(Glu-Glu-*N*-methyl)-1*H*-1,2,3-triazole (3b)**

971 1-(Tri-*O*-methyl-cellulosyl)-4-[Fmoc-Glu(*O**t*-Bu)-Glu(*O**t*-Bu)-*N*-methyl]-1*H*-  
972 1,2,3-triazole (161 mg) was dissolved in piperidine/dichloromethane (1/1, v/v, 2  
973 mL). The reaction mixture was stirred at room temperature for 4 h under nitrogen,

974 after which it was concentrated and purified by gel-filtration column  
975 chromatography (LH-60, eluent: 20% MeOH/CH<sub>2</sub>Cl<sub>2</sub>), and then by PTLC (eluent:  
976 10% MeOH/CH<sub>2</sub>Cl<sub>2</sub>) to give 1-(tri-*O*-methylcellulosyl)-4-[Glu(*O*-*t*-Bu)-Glu(*O*-*t*-  
977 Bu)-*N*-methyl]-1*H*-1,2,3-triazole (136 mg, 84% yield; GPC analysis:  $M_n =$   
978  $8.0 \times 10^3$ ,  $M_w / M_n = 1.6$ ).

979 1-(Tri-*O*-methylcellulosyl)-4-[Glu(*O*-*t*-Bu)-Glu(*O*-*t*-Bu)-*N*-methyl]-1*H*-1,2,3-  
980 triazole (124 mg) was dissolved in trifluoroacetic acid/distilled water (9/1, v/v, 1  
981 mL). The reaction mixture was stirred at room temperature for 4 h under nitrogen  
982 atmosphere, concentrated, and then purified by gel-filtration column  
983 chromatography (LH-60, eluent: 20% MeOH/CH<sub>2</sub>Cl<sub>2</sub>), and further purified by  
984 PTLC) eluent: 10% MeOH/CH<sub>2</sub>Cl<sub>2</sub>). The water-soluble component was collected  
985 by removal of the water-insoluble component by filtration, and concentrated to  
986 give 1-(tri-*O*-methylcellulosyl)-4-(Glu-Glu-*N*-methyl)-1*H*-1,2,3-triazole (**3b**, 64  
987 mg, 52% yield; GPC analysis:  $M_n = 7.0 \times 10^3$ ,  $M_w / M_n = 1.6$ ).

988 <sup>1</sup>H-NMR (500 MHz, D<sub>2</sub>O):  $\delta$  3.14 (t,  $J = 9.0$  Hz, H2<sub>Me</sub>), 3.40 (s, OMe), 3.45 (t,  $J$   
989  $= 9.0$  Hz, H3<sub>Me</sub>), 3.57 (s, OMe), 3.58 (s, OMe), 3.57-3.62 (H5<sub>Me</sub>), 3.60-3.82 (H4<sub>Me</sub>,  
990 H6<sub>Me</sub>), 4.43 (d,  $J = 8.0$  Hz, H1<sub>Me</sub>), 4.48 (d, 5.40 (d,  $J = 3.0$  Hz),  $J = 3.5$  Hz), 5.43  
991 (broad s), 8.43 (s, triazole *CH*)

992 FT-IR (KBr): 3460, 2928, 2836, 1732, 1626, 1458, 1377, 1310, 1126, 1084,  
993 1061, 945, 800, 704, 664, 571, 486 cm<sup>-1</sup>

## 994 Characterization

### 995 General

996 <sup>1</sup>H- and <sup>13</sup>C-NMR spectra were recorded on a Varian 500 NMR (500 MHz) or  
997 Varian INOVA300 (300 MHz) spectrometer in chloroform-*d* with  
998 tetramethylsilane as the internal standard, or in deuterium oxide with 3-

999 (trimethylsilyl)-1-propanesulfonic acid sodium salt as the external standard.  
1000 Chemical shifts ( $\delta$ ) and coupling constants ( $J$ ) are given in ppm and Hz,  
1001 respectively. Matrix-assisted laser-desorption/ionization time-of-flight mass  
1002 spectrometry (MALDI-TOF MS) was performed on a Bruker MALDI-TOF  
1003 Autoflex III mass spectrometer in positive ion and reflector or linear modes. A  
1004 smartbeam laser was used for ionization. All spectra were acquired in linear mode  
1005 and calibrated externally. 2,5-Dihydroxybenzoic acid was used as the matrix in  
1006 MALDI-TOF MS experiments. Shimadzu components, namely the liquid  
1007 chromatography injector (LC-10ATvp), column oven (CTO-10Avp), ultraviolet-  
1008 visible detector (SPD-10Avp), refractive index detector (RID-10A),  
1009 communication bus module (CBM-10A), and LC workstation (CLASS-LC10),  
1010 were used for HPLC separations, with Shodex columns (KF802, KF802.5, and  
1011 KF805). Number- and weight-averaged molecular weights ( $M_n$ ,  $M_w$ ) and  
1012 polydispersity indices ( $M_w/M_n$ ) were determined using polystyrene standards  
1013 (Shodex). A flow rate of 1 mL/min at 40 °C was chosen, and chloroform was used  
1014 as the eluent.

#### 1015 *Differential scanning calorimetry (DSC)*

1016 DSC thermograms were recorded on a DSC823<sup>e</sup> instrument (Mettler Toledo,  
1017 Zurich, Switzerland) with an HSS7 sensor under nitrogen during (0 → 90 → 0 °C)  
1018 heating/cooling cycles, with heating and cooling rates of 3.5 °C/min. Each  
1019 temperature cycle was repeated three times in order to ensure reproducibility.  
1020 Sample concentrations of 2.0 wt% were used in DSC experiments.

#### 1021 *Dynamic light scattering (DLS) experiments*

1022 DLS experiments were performed with an ELS-Z zeta-potential and particle-  
1023 size analyzer (Otsuka Electronics Co., Ltd, Osaka, Japan) and conducted in the



1024 10–90 °C temperature range. Sample solutions were maintained at the required  
1025 temperature for 5 min prior to each experiment. Sample concentrations of 0.2 wt%  
1026 were used in these experiments.

#### 1027 *Surface-tension measurements*

1028 Surface tensions were measured with a CBVP-A3 surface tensiometer (Kyowa  
1029 Interface Science, Co. Ltd., Tokyo, Japan) at 23 °C using the Wilhelmy method.  
1030 A Teflon cell containing 700 µL of the required solution was used in these  
1031 experiments. Surface tensions gradually decreased with time, and stable values  
1032 were recorded after 30 min.

#### 1033 *Scanning electron microscopy (SEM) and transmission electron* 1034 *microscopy (TEM)*

1035 The three hydrogels from aqueous solutions containing compounds **1b**, **2b**, and  
1036 **3b** were frozen in liquid nitrogen, lyophilized, and cut with a razor blade. The cut  
1037 surfaces of the hydrogels were sputter-coated with gold with an ion-coater (JFC-  
1038 1100E, JEOL, Tokyo, Japan) and examined by scanning electron microscopy  
1039 (SEM, JSM-6060, JEOL) at an accelerator voltage of 5 kV.

1040 A drop of an aqueous dispersion of compound **2b** was mounted on a copper grid  
1041 with an elastic carbon-support film (Oken Shoji, Tokyo, Japan) and examined by  
1042 transmission electron microscopy (TEM, JEM1400, JEOL) at an accelerator  
1043 voltage of 100 kV after negative staining with uranyl acetate.

#### 1044 *Release of model drugs from the thermoresponsive hydrogels*

1045 Compounds **2b** and **3b** (2 or 4 mg) were respectively added to glass vials  
1046 containing solutions of diclofenac sodium (DFNa) or imipramine hydrochloride  
1047 (IMC) (0.025 wt%) in PBS (100 µL), and the compounds were dissolved at about  
1048 0 °C. The glass vial was then heated at 37 °C for 10 min while left to stand. After

1049 a hydrogel had formed, a fresh PBS solution (500  $\mu$ L), which had been pre-heated  
1050 to 37 °C, was carefully poured onto the hydrogel surface. The glass vial was  
1051 shaken at 60 rpm in a water-bath shaker (Eyela NTS-4000, Tokyo Rikakikai Co.,  
1052 Ltd.). The aqueous layer (500  $\mu$ L) was then collected and filtered through a  
1053 membrane filter (pore size: 0.45  $\mu$ m). The UV absorbance of the aqueous solution  
1054 was recorded at 260 nm in a 96-well microplate using a SpectraMax Plus 384  
1055 Microplate Reader (Molecular Devices). The amount of released drug was  
1056 evaluated from the UV absorbance.

### 1057 *Cytotoxicity assays*

1058 Compounds **1b**, **2b**, and **3b** were dispersed in PBS at a concentration of 20  
1059 mg/mL and serially diluted by factors of two in a 96-well flat-bottomed plate (50  
1060  $\mu$ L/well (Corning Inc., Corning, NY). The human histiocytoma U937 cell line was  
1061 suspended in complete RPMI1640 medium at  $1 \times 10^4$  cells/mL and the cell  
1062 suspension was added to the 96-well flat bottom plate ( $5 \times 10^2$  cells/50  $\mu$ L/well).  
1063 The plate was incubated at 37 °C in a 5%-CO<sub>2</sub> atmosphere for 4 d. The plate was  
1064 allowed to stand at room temperature for 30 min, after which 100  $\mu$ L of CellTiter-  
1065 Glo Luminescent Cell Viability Assay reagent (Promega Corp., Madison, WI)  
1066 was added to each well. After thorough mixing, the contents of each well were  
1067 transferred into an Optiplate<sup>TM</sup>-96 multi-well plate (Perkin Elmer, Waltham, MA).  
1068 Cell viability was determined by measuring luminescence with an ARVO<sup>TM</sup> SX  
1069 Delfia 1420 Multilabel Counter (Perkin Elmer Life and Analytical Sciences,  
1070 Shelton, CT).

1071

1072 **Acknowledgements** This work was supported in part by JSPS Grants-in-Aid for Scientific  
1073 Research (B) nos. 24380092 and 15H04531.

1074

1075

## 1076 References

- 1077 Aagren JKM, Billing JF, Grundberg HE, Nilsson UJ (2006) Synthesis of a chiral and fluorescent  
1078 sugar-based macrocycle by 1,3-dipolar cycloaddition *Synthesis*:3141-3145 doi:10.1055/s-  
1079 2006-942503
- 1080 Akiyoshi K, Kohara M, Ito K, Kitamura S, Sunamoto J (1999) Enzymic synthesis and  
1081 characterization of amphiphilic block copolymers of poly(ethylene oxide) and amylose  
1082 *Macromol Rapid Commun* 20:112-115 doi:10.1002/(SICI)1521-  
1083 3927(19990301)20:3<112::AID-MARC112>3.0.CO;2-Q
- 1084 Baumann MD, Kang CE, Stanwick JC, Wang Y, Kim H, Lapitsky Y, Shoichet MS (2009) An  
1085 injectable drug delivery platform for sustained combination therapy *J Controlled Release*  
1086 138:205-213 doi:10.1016/j.jconrel.2009.05.009
- 1087 Bodvik R et al. (2010) Aggregation and network formation of aqueous methylcellulose and  
1088 hydroxypropylmethylcellulose solutions *Colloids Surf, A* 354:162-171  
1089 doi:10.1016/j.colsurfa.2009.09.040
- 1090 Bonduelle C, Lecommandoux S (2013) Synthetic Glycopolypeptides as Biomimetic Analogues of  
1091 Natural Glycoproteins *Biomacromolecules* 14:2973-2983 doi:10.1021/bm4008088
- 1092 Breitenbach BB, Schmid I, Wich PR (2017) Amphiphilic Polysaccharide Block Copolymers for  
1093 pH-Responsive Micellar Nanoparticles *Biomacromolecules* 18:2839-2848  
1094 doi:10.1021/acs.biomac.7b00771
- 1095 Dax D, Xu C, Langvik O, Hemming J, Backman P, Willfoer S (2013) Synthesis of SET-LRP-  
1096 induced galactoglucomannan-diblock copolymers *J Polym Sci, Part A: Polym Chem*  
1097 51:5100-5110 doi:10.1002/pola.26942
- 1098 de Medeiros Modolon S, Otsuka I, Fort S, Minatti E, Borsali R, Halila S (2012) Sweet Block  
1099 Copolymer Nanoparticles: Preparation and Self-Assembly of Fully Oligosaccharide-  
1100 Based Amphiphile *Biomacromolecules* 13:1129-1135 doi:10.1021/bm3000138
- 1101 Desbrieres J, Hirrien M, Rinaudo M (1998) A calorimetric study of methylcellulose gelation  
1102 *Carbohydr Polym* 37:145-152
- 1103 Du X, Zhou J, Shi J, Xu B (2015) Supramolecular Hydrogelators and Hydrogels: From Soft Matter  
1104 to Molecular Biomaterials *Chemical Reviews* 115:13165-13307  
1105 doi:10.1021/acs.chemrev.5b00299
- 1106 Fajardo AR, Guerrey A, Britta EA, Nakamura CV, Muniz EC, Borsali R, Halila S (2014) Sulfated  
1107 Glycosaminoglycan-Based Block Copolymer: Preparation of Biocompatible Chondroitin  
1108 Sulfate-b-poly(lactic acid) Micelles *Biomacromolecules* 15:2691-2700  
1109 doi:10.1021/bm5005355
- 1110 Fundueanu G, Constantin M, Ascenzi P (2009) Poly(N-isopropylacrylamide-co-acrylamide) cross-  
1111 linked thermoresponsive microspheres obtained from preformed polymers: influence of  
1112 the physico-chemical characteristics of drugs on their release profiles *Acta Biomater*  
1113 5:363-373 doi:10.1016/j.actbio.2008.07.011
- 1114 Heymann E (1935) Studies on sol-gel transitions. 1. The inverse sol-gel transformation of  
1115 methylcellulose in water *Trans Faraday Soc* 31:846
- 1116 Hung C-C et al. (2017) Conception of Stretchable Resistive Memory Devices Based on  
1117 Nanostructure-Controlled Carbohydrate-block-Polyisoprene Block Copolymers *Adv*  
1118 *Funct Mater* 27:n/a doi:10.1002/adfm.201606161
- 1119 Kamitakahara H, Baba A, Yoshinaga A, Suhara R, Takano T (2014) Synthesis and crystallization-  
1120 induced microphase separation of cellulose triacetate-block-poly(  $\gamma$  -benzyl-L-glutamate)  
1121 *Cellulose (Dordrecht, Neth)* 21:3323-3338 doi:10.1007/s10570-014-0383-3
- 1122 Kamitakahara H, Funakoshi T, Nakai S, Takano T, Nakatsubo F (2009a) Syntheses of 6-O-  
1123 ethyl/methyl-celluloses via ring-opening copolymerization of 3-O-benzyl-6-O-  
1124 ethyl/methyl- $\alpha$ -D-glucopyranose 1,2,4-orthopivalates and their structure-property  
1125 relationships *Cellulose* 16:1179-1185 doi:10.1007/S10570-009-9339-4
- 1126 Kamitakahara H, Funakoshi T, Takano T, Nakatsubo F (2009b) Syntheses of 2,6-O-alkyl  
1127 celluloses: Influence of methyl and ethyl groups regioselectively introduced at O-2 and  
1128 O-6 positions on their solubility *Cellulose* 16:1167-1178
- 1129 Kamitakahara H, Koschella A, Mikawa Y, Nakatsubo F, Heinze T, Klemm D (2008a) Syntheses  
1130 and comparison of 2,6-di-O-methyl celluloses from natural and synthetic celluloses  
1131 *Macromolecular Bioscience* 8:690-700

- 1132 Kamitakahara H, Murata-Hirai K, Tanaka Y (2012) Synthesis of blockwise alkylated  
1133 tetrasaccharide-organic quantum dot complexes and their utilization for live cell labeling  
1134 with low cytotoxicity *Cellulose* 19:171-187 doi:Doi 10.1007/S10570-011-9619-7
- 1135 Kamitakahara H, Nakatsubo F (2010) ABA- and BAB-triblock cooligomers of tri-O-methylated  
1136 and unmodified cello-oligosaccharides: syntheses and structure-solubility relationship  
1137 *Cellulose* 17:173-186 doi:Doi 10.1007/S10570-009-9348-3
- 1138 Kamitakahara H, Nakatsubo F, Klemm D (2006) Block co-oligomers of tri-O-methylated and  
1139 unmodified cello-oligosaccharides as model compounds for methylcellulose and its  
1140 dissolution/gelation behavior *Cellulose* 13:375-392
- 1141 Kamitakahara H, Nakatsubo F, Klemm D (2007) New class of carbohydrate-based nonionic  
1142 surfactants: diblock co-oligomers of tri-O-methylated and unmodified cello-  
1143 oligosaccharides *Cellulose* 14:513-528
- 1144 Kamitakahara H, Nakatsubo F, Klemm D (2009c) Synthesis of methylated cello-oligosaccharides:  
1145 synthesis strategy for block-wise methylated cello-oligosaccharides *ACS Symp Ser*  
1146 1017:199-211 doi:10.1021/bk-2009-1017.ch011
- 1147 Kamitakahara H, Suhara R, Yamagami M, Kawano H, Okanishi R, Asahi T, Takano T (2016) A  
1148 versatile pathway to end-functionalized cellulose ethers for click chemistry applications  
1149 *Carbohydr Polym* 151:88-95 doi:10.1016/j.carbpol.2016.05.016
- 1150 Kamitakahara H, Yoshinaga A, Aono H, Nakatsubo F, Klemm D, Burchard W (2008b) New  
1151 approach to unravel the structure-property relationship of methylcellulose. Self-assembly  
1152 of amphiphilic block-like methylated cello-oligosaccharides *Cellulose* 15:797-801  
1153 doi:10.1007/s10570-008-9232-6
- 1154 Karakawa M, Mikawa Y, Kamitakahara H, Nakatsubo F (2002) Preparations of regioselectively  
1155 methylated cellulose acetates and their H-1 and C-13 NMR spectroscopic analyses *J*  
1156 *Polym Sci Pol Chem* 40:4167-4179
- 1157 Kato T, Yokoyama M, Takahashi A (1978) Melting temperatures of thermally reversible gels  
1158 *Colloid Polym Sci* 256:15-21
- 1159 Kunishima M, Kawachi C, Iwasaki F, Terao K, Tani S (1999a) Synthesis and characterization of  
1160 4-(4,6-dimethoxy-1,3,5-triazin-2-yl)-4-methylmorpholinium chloride *Tetrahedron Lett*  
1161 40:5327-5330 doi:10.1016/S0040-4039(99)00968-5
- 1162 Kunishima M, Kawachi C, Morita J, Terao K, Iwasaki F, Tani S (1999b) 4-(4,6-Dimethoxy-1,3,5-  
1163 triazin-2-yl)-4-methylmorpholinium chloride: an efficient condensing agent leading to the  
1164 formation of amides and esters *Tetrahedron* 55:13159-13170 doi:10.1016/S0040-  
1165 4020(99)00809-1
- 1166 Liu J-Y, Zhang L-M (2007) Preparation of a polysaccharide-polyester diblock copolymer and its  
1167 micellar characteristics *Carbohydr Polym* 69:196-201 doi:10.1016/j.carbpol.2006.09.009
- 1168 Loos K, Müller AHE (2002) New Routes to the Synthesis of Amylose-block-polystyrene Rod-  
1169 Coil Block Copolymers *Biomacromolecules* 3:368-373 doi:10.1021/bm0156330
- 1170 Lott JR, McAllister JW, Arvidson SA, Bates FS, Lodge TP (2013a) Fibrillar Structure of  
1171 Methylcellulose Hydrogels *Biomacromolecules* 14:2484-2488 doi:10.1021/bm400694r
- 1172 Lott JR, McAllister JW, Wasbrough M, Sammler RL, Bates FS, Lodge TP (2013b) Fibrillar  
1173 Structure in Aqueous Methylcellulose Solutions and Gels *Macromolecules (Washington,*  
1174 *DC, U S)* 46:9760-9771 doi:10.1021/ma4021642
- 1175 Morelli P, Matile S (2017) Sidechain Engineering in Cell-Penetrating Poly(disulfide)s *Helv Chim*  
1176 *Acta* 100:e1600370 doi:10.1002/hlca.201600370
- 1177 Nakagawa A, Fenn D, Koschella A, Heinze T, Kamitakahara H (2011a) Physical Properties of  
1178 Diblock Methylcellulose Derivatives with Regioselective Functionalization Patterns: First  
1179 Direct Evidence that a Sequence of 2,3,6-Tri-O-methyl-glucopyranosyl Units Causes  
1180 Thermoreversible Gelation of Methylcellulose *Journal of Polymer Science Part B-*  
1181 *Polymer Physics* 49:1539-1546 doi:Doi 10.1002/Polb.22343
- 1182 Nakagawa A, Fenn D, Koschella A, Heinze T, Kamitakahara H (2011b) Synthesis of Diblock  
1183 Methylcellulose Derivatives with Regioselective Functionalization Patterns *J Polym Sci*  
1184 *Pol Chem* 49:4964-4976 doi:Doi 10.1002/Pola.24952
- 1185 Nakagawa A, Ishizu C, Sarbova V, Koschella A, Takano T, Heinze T, Kamitakahara H (2012a) 2-  
1186 O-Methyl- and 3,6-Di-O-methyl-cellulose from Natural Cellulose: Synthesis and  
1187 Structure Characterization *Biomacromolecules* 13:2760-2768 doi:Doi  
1188 10.1021/Bm300754u
- 1189 Nakagawa A, Kamitakahara H, Takano T (2011c) Synthesis of blockwise alkylated (1->4) linked  
1190 trisaccharides as surfactants: influence of configuration of anomeric position on their  
1191 surface activities *Carbohydr Res* 346:1671-1683 doi:10.1016/j.carres.2011.04.034

- 1192 Nakagawa A, Kamitakahara H, Takano T (2012b) Synthesis and thermoreversible gelation of
- 1193 diblock methylcellulose analogues via Huisgen 1,3-dipolar cycloaddition *Cellulose*
- 1194 19:1315-1326 doi:10.1007/S10570-012-9703-7
- 1195 Nakagawa A, Steiniger F, Richter W, Koschella A, Heinze T, Kamitakahara H (2012c)
- 1196 Thermoresponsive Hydrogel of Diblock Methylcellulose: Formation of Ribbonlike
- 1197 Supramolecular Nanostructures by Self-Assembly *Langmuir* 28:12609-12618
- 1198 Otsuka I, Osaka M, Sakai Y, Travelet C, Putaux J-L, Borsali R (2013) Self-Assembly of
- 1199 Maltoheptaose-block-Polystyrene into Micellar Nanoparticles and Encapsulation of Gold
- 1200 Nanoparticles *Langmuir* 29:15224-15230 doi:10.1021/la403941v
- 1201 Otsuka I, Travelet C, Halila S, Fort S, Pignot-Paintrand I, Narumi A, Borsali R (2012)
- 1202 Thermoresponsive Self-Assemblies of Cyclic and Branched Oligosaccharide-block-
- 1203 poly(N-isopropylacrylamide) Diblock Copolymers into Nanoparticles
- 1204 *Biomacromolecules* 13:1458-1465 doi:10.1021/bm300167e
- 1205 Parker J, Mitrousis N, Shoichet MS (2016) Hydrogel for Simultaneous Tunable Growth Factor
- 1206 Delivery and Enhanced Viability of Encapsulated Cells in Vitro *Biomacromolecules*
- 1207 17:476-484 doi:10.1021/acs.biomac.5b01366
- 1208 Rees DA (1972) Polysaccharide gels, A molecular view *Chem & Ind (London)* 19:630-636
- 1209 Sakai-Otsuka Y, Zaioncz S, Otsuka I, Halila S, Rannou P, Borsali R (2017) Self-Assembly of
- 1210 Carbohydrate-block-Poly(3-hexylthiophene) Diblock Copolymers into Sub-10 nm Scale
- 1211 Lamellar Structures *Macromolecules* 50:3365-3376 doi:10.1021/acs.macromol.7b00118
- 1212 Savage AB (1957) Temperature-Viscosity Relationships for Water-Soluble Cellulose Ethers *Ind*
- 1213 *Eng Chem* 49:99
- 1214 Schamann M, Schafer HJ (2003) TEMPO-mediated anodic oxidation of methyl glycosides and 1-
- 1215 methyl and 1-azido disaccharides *Eur J Org Chem*:351-358 doi:10.1002/ejoc.200390041
- 1216 Togashi D, Otsuka I, Borsali R, Takeda K, Enomoto K, Kawaguchi S, Narumi A (2014)
- 1217 Maltopentaose-Conjugated CTA for RAFT Polymerization Generating Nanostructured
- 1218 Bioresource-Block Copolymer *Biomacromolecules* 15:4509-4519
- 1219 doi:10.1021/bm501314f
- 1220 Yagi S, Kasuya N, Fukuda K (2010) Synthesis and characterization of cellulose-b-polystyrene
- 1221 *Polym J (Tokyo, Jpn)* 42:342-348 doi:10.1038/pj.2009.342
- 1222 Yamagami M, Kamitakahara H, Yoshinaga A, Takano T (2018) Thermo-reversible
- 1223 supramolecular hydrogels of trehalose-type diblock methylcellulose analogues *Carbohydr*
- 1224 *Polym* 183:110-122 doi:10.1016/j.carbpol.2017.12.006
- 1225 Yang HW, Yi JW, Bang E-K, Jeon EM, Kim BH (2011) Cationic nucleolipids as efficient siRNA
- 1226 carriers *Org Biomol Chem* 9:291-296 doi:10.1039/C0OB00580K
- 1227 Ying LQ, Gervay-Hague J (2003) General methods for the synthesis of glycopyranosyluronic acid
- 1228 azides *Carbohydr Res* 338:835-841 doi:10.1016/S0008-6215(03)00042-9
- 1229 Yu G-J, Chen X-Y, Mao S-Z, Liu M-L, Du Y-R (2017) Hydrophobic terminal group of surfactant
- 1230 initiating micellization as revealed by <sup>1</sup>H NMR spectroscopy *Chin Chem Lett* 28:1413-
- 1231 1416 doi:10.1016/j.cclet.2017.04.013
- 1232